POLITECNICO DI TORINO
Repository ISTITUZIONALE

A review on the heat and mass transfer phenomena in nanofluid coolants with special focus on automotive applications

Terms of use:

Publisher copyright

(Article begins on next page)

21 December 2024

A review on the heat and mass transfer phenomena in nanofluid coolants with special focus on automotive applications

Masoud Bozorg Bigdeli[a], Matteo Fasano[a], Annalisa Cardellini[a], Eliodoro Chiavazzo[a,*], Pietro Asinari[a]

[a]*Dipartimento di Energia, Politecnico di Torino, Corso Duca degli Abruzzi 24, 10129 Torino, Italy*

Abstract

Engineered suspensions of nanosized particles (nanofluids) may be characterized by enhanced thermal properties. Due to the increasing need for ultrahigh performance cooling systems, nanofluids have been recently investigated as next-generation coolants for car radiators. However, the multi-scale nature of nanofluids implies nontrivial relations between their design characteristics and the resulting thermo-physical properties, which are far from being fully understood. In this work, the role of fundamental heat and mass transfer mechanisms governing thermo-physical properties of nanofluids is reviewed, both from experimental and theoretical point of view. Particular focus is devoted to highlight the advantages of using nanofluids as coolants for automotive heat exchangers, and a number of design guidelines is reported for balancing thermal conductivity and viscosity enhancement in nanofluids. We hope this review may help further the translation of nanofluid technology from small-scale research laboratories to industrial application in the automotive sector.

*Corresponding author

Email address: eliodoro.chiavazzo@polito.it (Eliodoro Chiavazzo)

1. Introduction

In automotive liquid-cooled engines, radiator is a compact heat exchanger coupled to channels distributed throughout the cylinder heads and engine, through which the coolant is pumped. Different methods have been proposed to enhance the heat transfer performance of car radiators, and they can be classified into active and passive techniques [1, 2]. While active methods require power supply (e.g. mechanical mixing), passive enhancement techniques are not dependent on external sources and thus are characterized by lower operating costs and higher reliability, especially with compact energy devices [3, 4].

Among other passive methods such as fins, engineered surface texturing and microchannels [5–9], the adoption of novel coolants with enhanced thermo-physical properties as compared to conventional ones (e.g. water, oil, ethylene glycol) has attracted interest in the automotive field for a long time [10–16]. As a matter of fact, early scientists tried to suspend millimeter- and micrometer-sized particles with high thermal conductivity in traditional coolants to improve their thermal properties. However, due to the associated high pressure drop, clogging of flow channels and corrosion of the components (heat exchangers, pipelines, pumps), the approach was initially considered inappropriate. Later on, advancements in colloid and interface science along with improvements in powder manufacturing techniques resulted in the synthesis of colloidal suspensions of nanosized particles with enhanced transport properties, called nanofluids [17, 18].

2

In the past decades, nanofluids have been proposed for a wide variety of applications. In the engineering field, nanofluids have been mainly indicated as novel coolants for both electronic [19, 20] and automotive components [21–27], with the potential to reduce the dimensions of traditional heat exchangers. Nanofluids have also mechanical applications as magnetic sealants [28] or lubricants [29, 30], and energy applications in solar water heaters [21, 31]. More generally, nanofluids also show great potential in the biomedical sector, especially in antibacterial [32], nanocryosurgery [33] or theranostic [34, 35] applications.

The growing interest of automotive industry on nanofluid coolants is witnessed by the exponential increase of published patents and by market reports, which are indicating nanofluids as one of the key trends and drivers in the car radiator industry in the period 2014-2020 [36]. The main advantage of nanofluids for automotive cooling systems is the high thermal conductivity of solid nanoparticles, which can be hundreds or thousands times greater than the one of conventional heat transfer fluids [37, 38]. Therefore, nanofluids containing a small amount of uniformly and stably dispersed nanoparticles can provide a considerable enhancement in thermal conductivity (e.g. up to 30% increase with TiO_2-water suspensions [39, 40]) when compared to base fluids, such as water, ethylene glycol, engine oil or ethanol [41, 42]. However, the increased thermal conductance of nanofluids is often accompanied by increased viscosity and corrosion of mechanical components, therefore limiting a wider commercial exploitation of nanofluids in automotive applications [1].

If nanofluids are used as coolants in car radiators, a number of thermophysical properties have to be taken into account for evaluating their overall cooling efficiency, namely thermal conductivity, specific heat capacity,

density and viscosity [43]. This is because they strongly influence the characteristic thermal transmittance and inertia of the nanofluid as well as the required pumping power, respectively. However, an overall guideline for automotive engineers to provide them with the necessary tools to systematically analyze the influence of nanoparticles and base fluid parameters on the effective thermo-physical properties of nanofluid coolants, and subsequently on the engine performance, is still missing.

Thus, the approach towards the production of highly efficient engines necessitates the introduction of innovative cooling technologies, such as nanofluid coolants. However, it is essential to consider the effect of both increased thermal conductivity and viscosity to evaluate the global energy performance of nanofluid coolants. To this purpose, this review aims at rationalizing the experimental, computational and physical evidences on the heat and mass transfer phenomena observed in nanofluids. Furthermore, the potential heat transfer enhancement offered by nanofluids as novel coolants for automotive applications is critically reviewed. Finally, the challenges to harnessing the benefits of this technology are discussed and perspectives for further development of nanofluid technology are suggested.

2. Nanofluid synthesis

Nanofluids are suspensions of nanoparticles (diameter $d_p \leq 100$ nm) immersed in a host fluid also referred to as base fluid. Thermo-physical properties of nanofluids depend on the characteristics of base fluid and nanoparticles, which are both influenced by fabrication techniques. Nanoparticles are typically made out of a solid core and a shell or coating, which is chemically bonded or adsorbed on its surface. Generally, the nanoparticle core defines

the main characteristics of the particle, such as thermal, electric, magnetic and optical properties, whereas the nanoparticle coating defines the stability of the particle suspension as well as the hydrophilic or hydrophobic behavior and the interfacial Kapitza thermal resistance [44].

Thermo-physical properties of nanofluids have a strong dependence on the characteristics of host fluid [45]. Fluids like water, ethylene glycol, engine oil or a mixture of them are typically used for experiments on vehicle cooling systems [23, 26]. According to the hydrophilic or hydrophobic properties of both nanoparticle and host fluid, proper coatings and stabilizers should be employed to obtain stable suspensions [46].

Typical materials of nanoparticle core are ceramic (CuO, Al_2O_3, TiO_2, SiC, SiO_2, Fe_3O_4, ZnO), metallic (Cu, Al, Ag, Au, Fe) or carbon-based (carbon nanotube, graphene), whereas coatings may have molecular or polymeric composition [47–50]. Particle coatings may be in turn composed by an active head and a tail group, as schematically reported in Fig. 1. Generally, the active head group binds to the nanoparticle surface by creating chemical bonds: the stronger the chemical bonds are, the harder they tend to dissociate from the surface. This induces more stable nanofluid properties. The tail group, instead, is usually composed of two parts: a hydrocarbon chain and an ending tail. The tail group interacts with the dispersion medium, thus promoting a good dispersion of nanoparticles.

For instance, carbon nanotubes (CNTs) possess hydrophobic surface properties and, therefore, are prone to aggregation and sedimentation in aqueous media. For better stability in water, surface properties of CNTs are usually modified by introducing proper stabilizers, such as Sodium Dodecyl Sulfate (SDS) [51, 52]. On the other hand, metallic and ceramic nanoparticles are generally characterized by hydrophilic surface properties, and there-
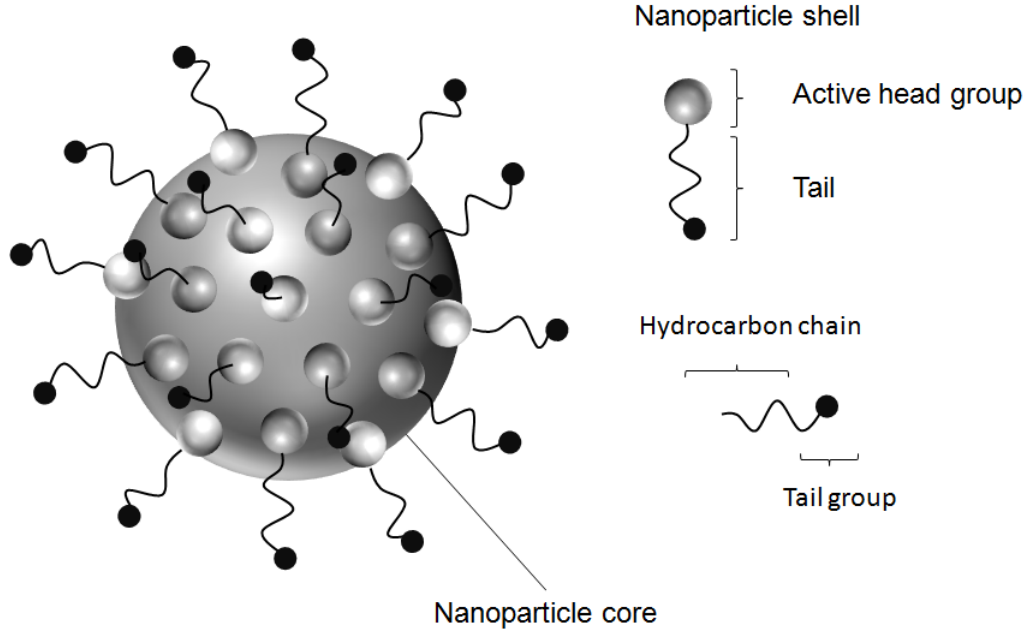
5

Figure 1: Schematic of a typical nanoparticle structure. Figure reproduced based on reference [47].

fore they should be functionalized for synthesizing stable oil-based nanofluids. Choi et al. [53] modified the Al_2O_3 nanoparticle surface by Oleic Acid (OA) through a hydrophobic modification process to prepare an oil-based nanofluid. As another example, Shima and Philip [54] modified Fe_3O_4 and Ag nanoparticles surfaces by Oleic Acid and Oleylamine, respectively, in order to prepare hexadecane-based nanofluids.

Two main methods are currently adopted for synthesizing nanofluids: single-step and two-step processes. In general, single-step synthesis is more reliable for producing metallic nanofluids, since it prevents particle oxidation. On the contrary, two-step technique is preferable for the synthesis of ceramic-based (e.g. oxides, carbides) nanofluids [46, 55].

6

Single-step synthesis can be performed by either physical [56] or chemical methods [57]. Introduced by Akoh et al. [56], the single-step physical synthesis involves the direct condensation of metallic vapor into nanoparticles by contact with a low vapor pressure fluid flow [58]. Generally, single-step processes directly synthesize nanoparticles in the base fluid, thus avoiding the processes of drying storage, transportation and re-dispersion of the metallic nanoparticles [57, 59]. Normally, physical vapor deposition [56, 58], solution chemical method [57] or microwave-assisted route [60, 61] are adopted for single-step synthesis of nanofluids. These methods usually minimize agglomeration of particles in the nanofluid and thus enhance its stability. However, single-step methods introduce a limit to the nanofluid production quantities, because only low vapor pressure liquids are currently compatible with these processes [62, 63].

Two-step methods are also widely used for the synthesis of nanofluids. In these processes, the dry nanopowders available from different physical and chemical methods (e.g. inert gas condensation [64], chemical vapor deposition [65, 66], physical vapor deposition [67] or mechanical alloying [68]) are dispersed into a base fluid [69–72]. Currently, the two-step approach is the cheaper method for large scale production of nanofluids, since nanopowder synthesis techniques have already been scaled up to industrial production levels. Moreover, two-step processes are widely adopted also because of the possibility to precisely and easily control the concentration and size distribution of the solvated nanoparticles [73, 74]. The main drawback of two-step techniques is the higher possibility of particle agglomeration due to attractive van der Waals interactions [55, 75].

Ultrasonic agitation as well as pH adjustment or introduction of surfactants may be required to obtain stable suspensions [69, 72, 76, 77]. In

detail, surface active agents (i.e. surfactants) are molecular structures with amphiphilic nature (i.e. coexistence of hydrophobic and hydrophilic molecular portions [78]), which makes them ideal stabilizers for nanofluids with aqueous or oleic phases. Surfactants can be introduced either during the fabrication process (two-step processes, Fig. 2) or directly into the synthesized nanofluid (single-step processes).
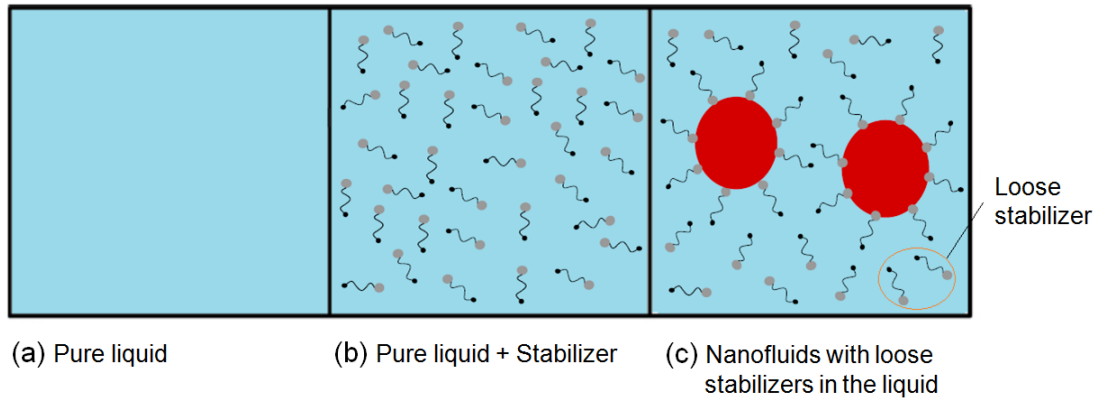

(a) Pure liquid   **(b)** Pure liquid + Stabilizer   **(c)** Nanofluids with loose stabilizers in the liquid

Figure 2: Two-step fabrication of nanofluids using stabilizers. Figure reproduced based on reference [1].

3. Dominating heat and mass flow mechanisms

The multiscale nature of nanofluids leads to nontrivial relations between their geometrical, physical and chemical characteristics and the resulting thermo-physical properties. This pronounced sensitivity is the main reason for some contradictory results among both experimental evidence and theoretical considerations presented in the literature.

In particular, classic effective medium theory has been modified to take into account the structured solid-like layer of water molecules at the nanoparticle-

fluid interface (i.e. nanolayer) [79–88]. Moreover, Brownian motion [89–94], interfacial thermal resistance (i.e. Kapitza Resistance) [95] and the formation of thermal percolation paths due to particle aggregation [96] were also proposed for understanding the anomalous thermal properties of nanofluids [38, 97–99]. After several experiments and some controversies, it is now well recognized that the two main features characterizing the effective thermal conductivity of nanofluids are the Kapitza resistance at the nanoparticle-fluid interface [100] as well as the role of aggregation and aggregate morphologies [101]. In particular, it is nowadays accepted that chain-forming morphologies of nanoparticles allow effective medium theories to predict thermal conductivity enhancements [102]. As a counter example, a large round-robin test on nanofluids proved that ideal dispersion cancels out any meaningful enhancement [103].

Experimental data corresponding to thermal conductivity of nanofluids largely fall within the lower and upper Maxwell bounds derived by Hashin and Shtrikman [104]. Most enhancements beyond predictions of effective medium theories come from thermal percolating effects due to aggregation of nanoparticles (see Fig. 3, where k_{nf} and k_{bf} are thermal conductivities of nanofluid and base fluid, respectively) [99]. The only way to benefit from the aggregation of nanoparticles while avoiding its negative effects is to have control over the entire process and keep aggregation at controlled levels. This is of prominent importance in automotive cooling circuits, as uncontrolled aggregation may lead to clogging of tubes. Understanding the nature of interaction forces between nanoparticles may pave the way to achieve control over this process.

Hence, the study of aggregate morphologies and dynamics is currently a central topic in colloidal science. The key tool for the molecular investigation
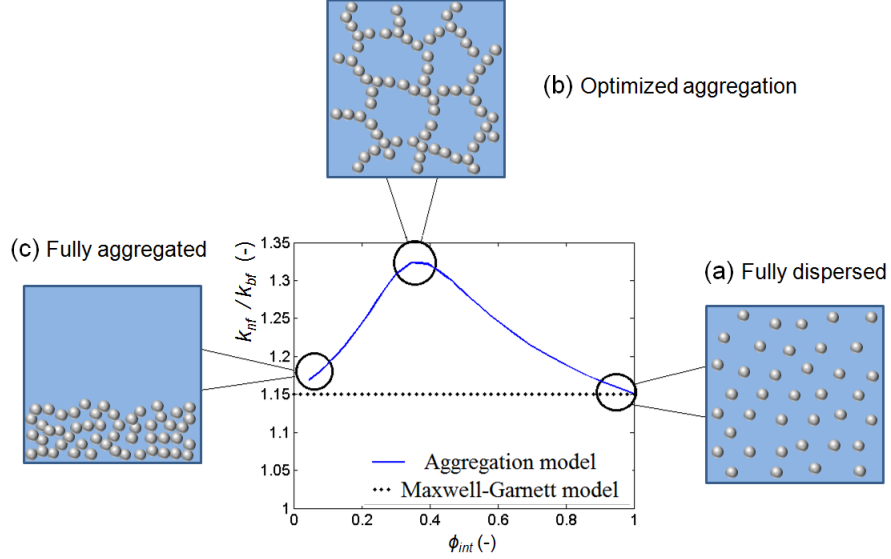
9

Figure 3: Aggregation dependence of thermal conductivity enhancement in nanofluids. (a) For a well-dispersed system, there is only one particle in each aggregate ($\phi_{int} = 1$) and the thermal conductivity is in accordance with effective medium theory (Maxwell-Garnett model [105]). (b) As particles tend to aggregate, the thermal conductivity of the suspension increases (diverges from Maxwell-Garnett model) and experiences a maximum value at optimized aggregation state. (c) Further aggregation increase leads to lower thermal conductivity values, until the system is fully-aggregated. Figure reproduced based on references [1, 98, 106].

of particle aggregation mechanisms is the effective interaction potential between nanoparticles, which can be qualitatively described by the well-known DLVO theory (due to Derjaguin, Landau, Verwey and Overbeek) [107–109]. However, it is nowadays recognized that additional forces (so called non-DLVO forces) play a major role in determining the colloidal stability [110]. Solvation forces, for example, can arise when liquid molecules are induced to order in the nanoscale gaps between approaching nanoparticles; however, fundamental theories are still missing for a more quantitative prediction of

10

non-DLVO forces and thus aggregation phenomena [110].

4. Thermal properties of nanofluids

Thermal conductivity (k_{nf}), specific heat capacity ($c_{p,nf}$) and thermal expansion (β_{nf}) can be considered as the main quantities for evaluating the overall thermal performance of nanofluids. Typically, thermal conductivity of nanofluids is larger than that of the base fluid, whereas specific heat capacity is smaller. In this section, thermal properties of nanofluids are reviewed from both experimental, modeling and theoretical point of view.

4.1. Thermal conductivity

4.1.1. Experimental evidences

Several techniques have been proposed for measuring thermal conductivity of nanofluids, namely transient methods, steady-state methods and the thermal comparator technique [111]. Transient approaches include transient hot-wire technique [39, 112–116], thermal constants analyzer [117, 118], temperature oscillation [119, 120] and the 3ω method [121]. Steady-state parallel-plate [122] and cylindrical cell [123] can be instead classified as steady-state techniques. Among these methods, transient hot-wire technique is the most adopted solution. Noteworthy, Li et al. [124] compared results from transient and steady-state thermal conductivity measurements in a Al$_2$O$_3$-water nanofluid. Results revealed that both methods led to similar thermal conductivity values at room temperature; whereas, by increasing temperatures, a significant discrepancy between the methods was evident. This was due to the onset of natural convection in the hot-wire setup [125].

Experimental analyses on thermal conductivity of nanofluids have shown several non-trivial characteristics. First, opposite trends are noticeable re-

11

garding the relation between thermal conductivity and decreasing particle size: (1) a decrease of thermal conductivity because of the increase in the overall solid-liquid interface effects [45, 126–131] (Fig. 4); (2) an increase of thermal conductivity because of the nanolayer effect and the increase of random motion of nanoparticles, which promotes the creation of percolation paths [89, 98, 132–134].
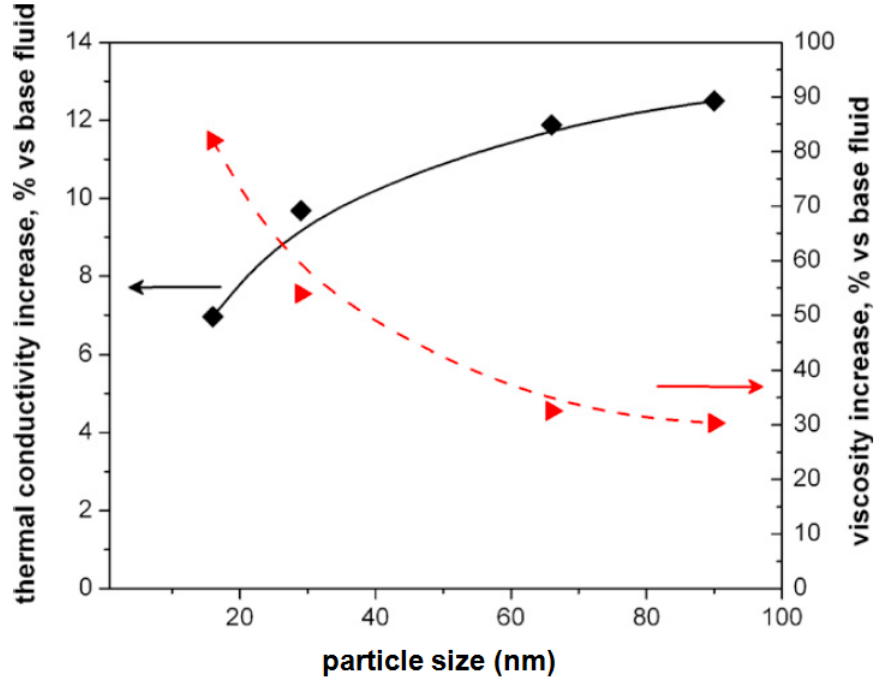
Figure 4: Dependence of thermal conductivity and viscosity of α-SiC-water nanofluids on the particle size ($T=22.5$°C, $\phi = 0.041$, pH=9.4). The black line and diamonds represent the dependence of k_r on d_p, whereas the red dashed line and triangles represent the dependence of μ_r on d_p. Figure adopted from reference [130].

Second, the pH of nanoparticle suspensions strongly affects the nanofluid stability and its thermo-physical properties. For heat transfer purposes, it

is generally recommended to synthesize suspensions with pH values far from isoelectric point (IEP), in order to avoid severe aggregation of nanoparticles [135]. Some studies underline an enhancement in thermal conductivity around the IEP [136–138], which could be due to the partial aggregation of particles and subsequent formation of thermal percolation pathways [98, 132, 133]. Therefore, a partial and controlled aggregation of nanoparticles, which can be adjusted by either pH tuning or surfactant addition, may enhance the thermal properties of nanofluids [77, 139–141].

Third, several experimental works report $k_r = k_{nf}/k_{bf}$ as a function of surfactant concentration. Based on these studies, there exists an optimum value at which k_r is maximum, as depicted in Fig. 5 [77, 118]. On one hand, this enhancement is due to a better dispersion of nanoparticles within the base fluid; on the other hand, it could be also attributed to nanolayer formation [117, 118].

Finally, thermal conductivity may show nonlinear behavior with particle concentration [142, 143], temperature dependence [119, 144–149] and the possibility to be tuned by external fields [150, 151].

Thermal conductivity values for a selection of nanoparticles, base fluids and nanofluids of interest for automotive applications are reported in Tables 1,2,3, respectively.

4.1.2. Semi-empirical models

Starting from experimental evidences, scientists have tried to semi-empirically model the relation between nanofluid characteristics and resulting thermal conductivity. For instance, the experimental model developed by Patel et

Table 1: Thermal conductivity (W/mK) of particle materials at 300 K.

Material	Thermal conductivity (W/mK)	References
MWCNT	3000	[48, 152]
Ag	429	[37, 152]
Cu	383-401	[37, 153]
Al	204-237	[152, 153]
Si	148	[37, 152]
SiC	120-490	[140, 152, 154]
CuO	18-76.5	[153, 155, 156]
Al_2O_3	40	[48]
SiO_2	1.38	[156]

Table 2: Thermal conductivity (W/mK) of heat transfer fluids at 27°C (unless otherwise noted). Water-EG is a 50:50 wt% mixture of water and ethylene glycol.

Fluid	Thermal conductivity (W/mK)	References
Water	0.613	[37, 152]
EG	0.253	[152]
EO	0.145	[37, 152]
Water-EG	0.403	[76, 157]
Water-EG at 90°C	0.422	[76]

Table 3: Thermal conductivity experimentally measured in nanofluids.

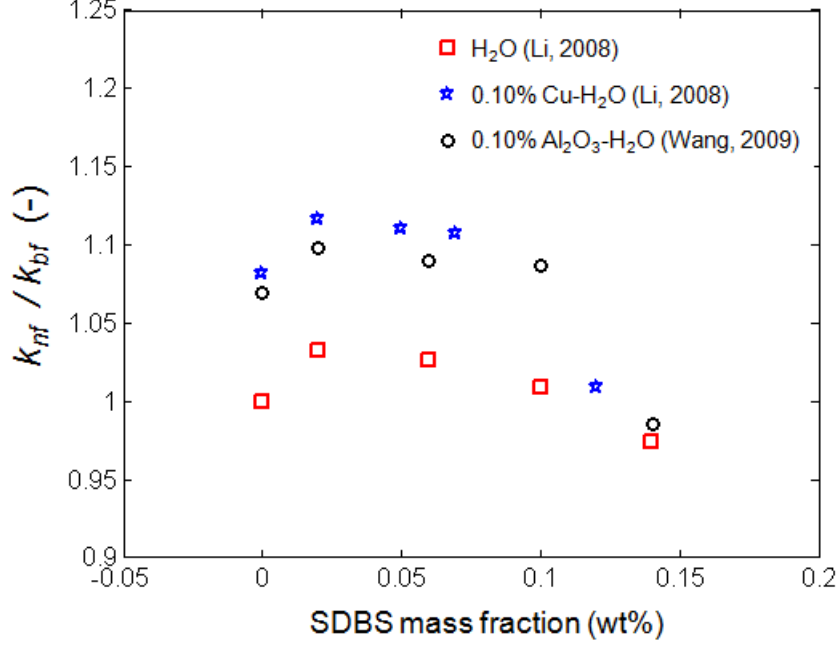| Nanofluid	Particle diameter (nm)	Particle length (nm)	ϕ (%)	Temperature (°C)	k_{nf} (W/mK)	References
Al_2O_3-Water	40	-	10	23	0.734	[158]
Al_2O_3-EG	40	-	10	23	0.312	[158]
Al_2O_3-Water/EG	10	-	2.9	23	0.468	[76]
CuO-Water	29	-	12	21 to 23	0.70	[147]
DWCNT-Water	3.5	$(1-10) \times 10^3$	0.14	-	0.8778	[159]
SWCNT-Water	1	100 to 600	0.2	60	0.756	[160]
SWCNT-EG	1	100 to 600	0.2	55	0.358	[160]

Figure 5: Effect of SDBS concentration on thermal conductivity of Cu- and Al_2O_3-water based nanosuspensions. Blue stars, black circles and red squares represent Al_2O_3-water suspensions, Cu-water suspensions and pure water, respectively. Figure is reproduced based on reference [118].

al. [153] for spherical metallic and oxide nanoparticle suspensions is:

$$k_r = \left(1 + 0.135 \times \frac{k_p}{k_{bf}}^{0.273} \right.$$
$$\left. \times \phi^{0.467} \times \frac{T}{20}^{0.547} \times \frac{100}{d_p}^{0.234}\right) \quad , \tag{1}$$

where T is the nanofluid temperature.

In another work, Corcione [161] proposed an empirical model based on data extracted from experimental studies:

$$k_r = 1 + 4.4 Re^{0.4} Pr^{0.66} \left(\frac{T}{T_{fr}}\right)^{10} \left(\frac{k_p}{k_{bf}}\right) \phi^{0.66} \quad , \tag{2}$$

15

where Re is the Reynolds number for the Brownian motion of nanoparticles, Pr is the Prandtl number of the base fluid and T_{fr} is the freezing point of the base fluid. This model is valid for water and ethylene glycol based nanofluids containing alumina, copper oxide, titania or copper nanoparticles. Re can be evaluated as:

$$Re = \frac{\rho_{bf} u_B d_p}{\mu_{bf}} \quad , \tag{3}$$

where u_B and μ_{bf} are the mean Brownian velocity of the nanoparticle and the viscosity of the base fluid, respectively; whereas Pr is defined as:

$$Pr = \frac{c_{p,bf} \mu_{bf}}{k_{bf}} \quad . \tag{4}$$

Chon et al. [162], instead, proposed an experimental correlation for the thermal conductivity of Al_2O_3 nanofluids based on Buckingham-Pi theorem:

$$k_r = 1 + 64.7\phi^{0.7460} \left(\frac{d_{bf}}{d_p}\right)^{0.3690}$$
$$\times \left(\frac{k_p}{k_{bf}}\right)^{0.7476} \times Pr^{0.9955} Re^{1.2321} \quad , \tag{5}$$

where d_{bf} is the base fluid molecule diameter.

Timofeeva et al. [163] experimentally proved that Kapitza resistance increases with decreasing particle sphericity, because of enhanced interfacial effects. Thus, they modeled the thermal conductivity of nanofluids by considering the effects of shape and thermal boundary resistance, namely:

$$k_r = 1 + (C_K{}^{shape} + C_K{}^{surface})\phi \quad , \tag{6}$$

where $C_K{}^{shape}$ is the contribution due to particle shape and $C_K{}^{surface}$ the contribution due to Kapitza resistance (Fig. 6). Based on this study, it is possible to define an upper limit for the shape factor of nanoparticles above which the limiting effect due to Kapitza resistance increases faster than the positive contribution by particle shape, namely $n < 5$.
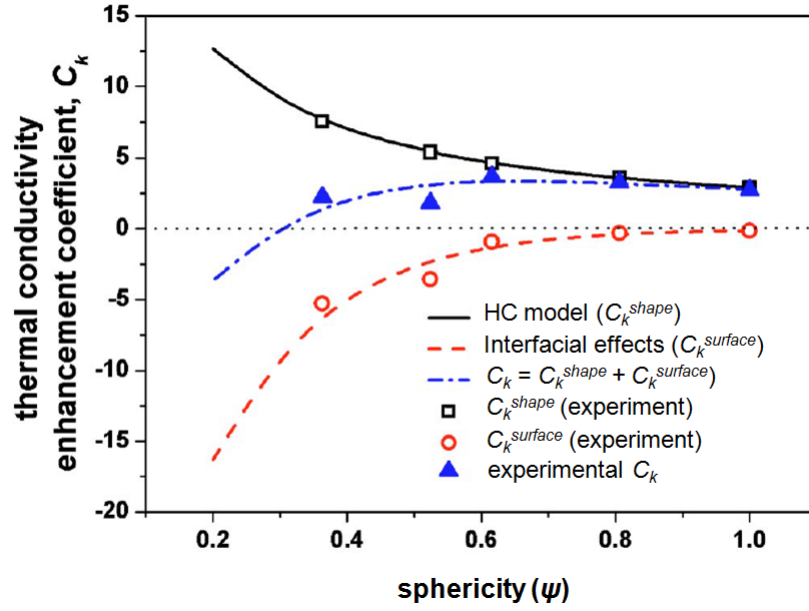
16

Figure 6: Contribution of particle shape and interfacial thermal resistance to the thermal conductivity of nanofluids at various particle sphericity (ψ). Black solid, red dashed and blue dash-dotted lines represent the Hamilton and Crosser - HC model, the trend of interfacial effects and the overall influence of shape and interface properties, respectively. Black squares, red circles and blue triangles represent the experimental evaluation of particle shape effect ($C_k{}^{shape}$), particle surface effect ($C_k{}^{surface}$) and their overall influence on thermal conductivity enhancement (C_k), respectively. Figure adopted from reference [163].

4.1.3. Theoretical models

To provide a mechanistic explanation of the thermal conductivity enhancement in nanofluids, various theoretical models based on classical effective medium theory (EMT) have been introduced, and some of them are discussed here.

The Maxwell-Garnett (MG) model [105] predicts the thermal conductivity enhancement (k_r) for a homogeneous suspension as:

$$k_r = \frac{k_{nf}}{k_{bf}} = \frac{k_p + 2k_{bf} + 2(k_p - k_{bf})\phi}{k_p + 2k_{bf} - (k_p - k_{bf})\phi} \quad , \tag{7}$$

where k_p is the particle thermal conductivity, whereas ϕ is the particle volume fraction. Note that, the maximum heat conduction enhancement ($k_{r,max}$) is obtained for $k_p >> k_{bf}$. This condition represents the upper limit for thermal conduction enhancement within the macroscopic theory [116], namely:

$$k_{r_{max}} = \frac{1 + 2\phi}{1 - \phi} \approx 1 + 3\phi \quad . \tag{8}$$

The MG model holds for low concentrations of not interacting spherical particles; therefore, it does not interpret experimental results at high volume concentrations. On the contrary, the Bruggeman model (BG) has no limitation on the spherical particles concentration, and it accounts for interactions among particles. This model can be expressed as:

$$\phi \left(\frac{k_p - k_{nf}}{k_p + 2k_{bf}} \right) + (1 - \phi) \left(\frac{k_{bf} - k_{nf}}{k_{bf} + 2k_{nf}} \right) = 0 \quad . \tag{9}$$

Note that, for low volume fractions, MG and BG models lead to approximately equal results [164, 165].

The Maxwell-Garnett model only considers volume concentration and thermal conductivity of particles and base fluid. Starting from MG relation,

Hamilton and Crosser (HC) [166] developed a model also taking into account the particle shape:

$$k_r = \frac{k_p + (n-1)k_{bf} - (n-1)(k_{bf} - k_p)\phi}{k_p + (n-1)k_{bf} + (k_{bf} - k_p)\phi} \quad . \tag{10}$$

where $n = 3/\psi$ is the shape factor and ψ the particle sphericity. The latter is defined as the ratio between the equivalent sphere surface and the actual particle surface, at fixed volume [163].

The MG and HC models are accurate to order ϕ^1. Jeffrey [167] extended the accuracy of these models to ϕ^2 for spherical nanoparticles, namely:

$$k_r = 1 + 3\beta\phi + \phi^2 \left(3\beta^2 + \frac{3\beta^2}{4} + \frac{9\beta^3}{16}\frac{\alpha + 2}{2\alpha + 3} + \frac{3\beta^4}{2^6} + ... \right), \tag{11}$$

where $\alpha = k_p/k_{bf}$ and $\beta = (\alpha - 1)/(\alpha + 2)$.

Further theoretical models were developed to explain the heat conduction behavior of nanofluids, thus giving rise to controversies and mismatch between experimental evidences and modeling interpretations [119, 144, 146, 149, 153, 158, 168, 169].

4.2. Other thermal properties

4.2.1. Specific heat capacity

Specific heat capacity, c_p, has received little attention if compared to thermal conductivity and viscosity of nanofluids. However, this quantity has an important role to define the thermal performance of nanofluids in cooling applications (see section 6), as it is incorporated into the energy equation [170, 171].

Differential Scanning Calorimeter (DSC) is recognized as the standard technique for measuring the specific heat capacity of fluids and materials. DSC technique has been successfully implemented in a large number of

nanofluid studies [172–178]. Alternatively, some researchers suggested their own experimental setups for measuring c_p of nanofluids [8, 179, 180].

In experiments, the specific heat capacity of nanofluids ($c_{p,nf}$) is found to be influenced by several parameters, including particle volume or weight fraction [69, 173, 174, 176, 177, 179, 181–183], temperature [176, 177, 181, 182, 184], particle size and shape [185], particle material [186], and base fluid type [186].

For instance, in the case of alumina nanoparticles in water, the increase in particle volume fraction induces a $c_{p,nf}$ decrease, because the specific heat capacity of alumina particles is lower than c_p of water [179, 187]. However, in case of carbon nanotubes (CNTs) in ethylene glycol (EG) the opposite behavior is observed, due to the higher specific heat capacity of CNT particles compared to that of EG [187, 188]. With respect to the particle size effect, Wang et al. [185] showed that $c_{p,p}$ depends on the size and shape of nanoparticles. Hence, it is also possible to tune $c_{p,nf}$ by adjusting nanoparticles' geometry.

Starting from the experimental data of Al_2O_3, SiO_2, and ZnO nanofluids, Vajjha and Das [179] developed a general correlation for $c_{p,nf}$:

$$c_{p,r} = \frac{c_{p,nf}}{c_{p,bf}} = \frac{(AT) + B(\frac{c_{p,p}}{c_{p,bf}})}{C + \phi} \quad , \tag{12}$$

where $c_{p,r}$ is the specific heat capacity ratio and A,B,C are fitting coefficients (see reference [179]). The latter correlation predicts the specific heat capacity of nanofluids for concentrations up to either 10% (Al_2O_3 and SiO_2 nanoparticles) or 7% (ZnO nanoparticles), within the temperature range of 315-363 K [179].

Two theoretical models based on mixing rules are generally adopted to predict the effective heat capacity of nanofluids ($c_{p,nf}$). Pak and Cho [69]

20

introduced the first model, namely:

$$c_{p,nf} = (1 - \phi)c_{p,bf} + \phi c_{p,p} \quad , \tag{13}$$

where $c_{p,bf}$ and $c_{p,p}$ are the base fluid and particle specific heat capacity, respectively. Therefore, in the case of aqueous nanofluids, $c_{p,nf}$ is reduced by increasing the nanoparticle volume concentration.

Assuming that nanoparticles and base fluid are in thermal equilibrium, Xuan and Roetzel [189] suggested a second model [189]:

$$c_{p,nf} = \frac{(1 - \phi)(\rho c_p)_{bf} + \phi(\rho c_p)_p}{\rho_{nf}} \quad , \tag{14}$$

where $(\rho c_p)_{bf}$ and $(\rho c_p)_p$ are the volumetric heat capacities of base fluid and nanoparticles, respectively, and ρ_{nf} is the nanofluid density. The latter model accurately predicts most experimental results and, hence, it is usually employed in nanofluid studies [180, 190, 191].

For extended reviews regarding the typical nanofluids specific heat capacity, the reader is delegated to references [175, 179, 190, 192].

4.2.2. Thermal expansion

The characteristic thermal expansion of a fluid also affects its heat transfer performances. Two theoretical models are widely used for predicting the effective thermal expansion coefficient of nanofluids (β_{nf}).

The first model is:

$$\beta_{nf} = (1 - \phi)\beta_{bf} + \phi\beta_p \quad , \tag{15}$$

where β_{bf} and β_p are the base fluid and nanoparticle thermal expansion coefficients, respectively [193]. In the second model, β_{nf} is approximated by a density-weighted average of particle and base fluid properties [194],

namely:

$$\beta_{nf} = \frac{(1 - \phi)(\rho\beta)_{bf} + \phi(\rho\beta)_p}{\rho_{nf}} \quad , \tag{16}$$

where ρ_{bf} and ρ_p are base fluid and nanoparticle density, respectively. Note that Eqs. (15) and (16) are analogous to the models adopted for the specific heat capacity of nanofluids, namely Eqs. (13) and (14).

However, these models are sometimes insufficient to accurately interpret experiments. For instance, Ho et al. [195] experimentally measured β_{nf} of alumina-water nanofluids at different volume fractions, finding that neither Eq. (13) nor (14) could fit well the $\phi - \beta$ relation [165].

5. Fluid dynamic properties of nanofluids

Fluid dynamic properties of nanofluids are other important factors to be considered in heat transfer applications. In this section, the relation between nanofluid characteristics, viscosity and density are reviewed.

5.1. Viscosity

5.1.1. Experimental evidences

Viscosity is usually measured by rotational [196], capillary [197] or piston-type [198] viscometers.

Rotational viscometers evaluate the fluid viscosity by measuring the torque required to turn an object in that fluid. Using this viscometer, the viscosity of both Newtonian and non-Newtonian fluids can be measured. However, the time consuming procedure (≈ 1 hour per sample) and the relatively large amount of sample consumptions ($\approx 1 \ mL$ per test) are the main drawbacks of employing rotational viscometers [199]. Moreover, classical models for the nanofluid viscosity [200, 201] often underpredict measurements by rotational viscometers [202]. Some researchers argued that

the difference between theoretical expectations and experimental results is associated with the low measurement accuracy of rotational viscometers, at least with nanofluid samples [202–204].

Therefore, capillary viscometers with different tube diameters are preferred in several experimental studies [202, 203]. The main drawback of capillary viscometers is the possible dependence of viscosity on the particle-to-tube ratio [203]. Furthermore, the uncertainties in the measurement of tube diameter size, pressure drop and flow rate may affect the overall accuracy of capillary viscometers [202, 204].

Experimental evidences on nanofluid viscosity (μ_{nf}) have shown a strong dependence on the physical and chemical properties of the suspension, such as nanoparticle size and shape [130][63, 163, 205–207], solid phase volume concentration [163, 208–210], pH of the solution [136, 211], surfactant concentration [78, 212–215] and temperature of the suspension [198, 216].

In particular, controversial trends concerning the effect of particle size on the effective viscosity of nanofluids are reported in the literature. Some scientists notice the increase of viscosity by reducing the particle size (Fig. 4) [45, 130, 217–219], whereas other studies report an opposite trend [198, 220]. The existence of these contradictory results could be due to several factors, such as different nanofluid preparation or measuring techniques, as well as presence of different surfactants, pH, temperature or agglomeration during the experiments [63, 130].

Extended reviews regarding experimental viscosity of nanofluids can be found in references [63, 210, 216, 221–225].

5.1.2. Semi-empirical models

Numerous empirical models have been formulated to interpret experimental results of nanofluids viscosity [165, 198, 218, 226–228].

For example, Yang et al. [172] studied the temperature dependence of viscosity, experimentally proving that viscosity decreases with increasing temperatures. In addition, Namburu et al. [229] observed that, in the range -35 to 50 °C, the viscosity of a nanofluid made out of CuO nanoparticles suspended in a 60:40 mixture of ethylene glycol and water has an exponential dependence with temperature, namely:

$$\log(\mu_{nf}) = A \exp(-BT) \quad , \tag{17}$$

where the coefficients A and B are function of ϕ.

Khanafer and Vafai [165], instead, analyzed the viscosity of Al_2O_3-water nanofluids from the experimental data available in the literature [69, 198, 230, 231]. The following empirical correlation was proposed as best fitting of literature results:

$$\mu_{nf} = -0.4491 + \frac{28.837}{T} + 0.574\phi - 0.1634\phi^2 +$$
$$+ \frac{23.053\phi^2}{T^2} + 0.0132\phi^3 - \frac{2354.735\phi}{T^3} +$$
$$+ \frac{23.498\phi^2}{d_p^2} - \frac{3.0185\phi^3}{d_p^2} \quad , \tag{18}$$

with $1\% \leq \phi \leq 9\%$, 20°C $\leq$ T $\leq$ 70°C and 13 nm $\leq d_p \leq$ 131 nm.

Rudyak and Krasnolutskii [219] numerically estimated the viscosity of suspensions of aluminum and lithium nanoparticles (d_p=2 nm, T=300 K) in liquid argon as a function of nanoparticle size and material. Results revealed that the viscosity of the nanofluid had a quadratic dependence on

24

the volume concentration:

$$\mu_r = 1 + a_1\phi + a_2\phi^2 \quad, \tag{19}$$

where a_1=3.20 and a_2=25.38 for Li nanoparticles, whereas a_1=3.25 and a_2=13.06 for Al nanoparticles. Rudyak and Krasnolutskii also found that viscosity increases with decreasing nanoparticle size:

$$\mu_r = \mu_{r,B} + (5.25\phi + 40.94\phi^2)\exp(-0.208d_p/d_{bf}) \quad, \tag{20}$$

where $\mu_{r,B}$ is calculated according to the Batchelor's relation [232] in Eq. (24), with d_p=1-4 nm and $\phi = 0.1 - 0.12$.

5.1.3. Theoretical models

Several theoretical models have been introduced to model the dependence of nanofluid viscosity with the fluid characteristics and parameters [200, 201, 232–239].

First, the Einstein model [200] for infinitely dilute suspensions ($\phi \leq 0.02$) containing spherical particles is formulated as:

$$\mu_r = \frac{\mu_{nf}}{\mu_{bf}} = (1 + 2.5\phi) \quad, \tag{21}$$

being μ_r the enhanced viscosity ratio, μ_{bf} and μ_{nf} the effective viscosity of base fluid and nanofluid, respectively.

Brinkman [233] extended Einstein model to larger volume concentrations ($\phi < 0.04$):

$$\mu_r = \frac{\mu_{nf}}{\mu_{bf}} = \frac{1}{(1 - \phi)^{2.5}} = 1 + 2.5\phi + 4.375\phi^2 + ... \quad. \tag{22}$$

Lundgren [234] tried to generalize the Brinkman's method by proposing a Taylor series expansion, which is valid for the case of spherical particles

suspensions and $\phi < 0.35$:

$$\mu_r = \frac{1}{1 - 2.5\phi} = 1 + 2.5\phi + 6.25\phi^2 + ... \quad . \tag{23}$$

At low volume fractions, the second (or higher) orders of ϕ become negligible; therefore, Lundgren's model reduces to Einstein's model. Furthermore, Batchelor [232] considered the effect of both hydrodynamic interactions and Brownian motion of particles on the viscosity of homogeneous suspensions of spherical particles, and a relation similar to the Lundgren's model has been obtained:

$$\mu_r = 1 + 2.5\phi + 6.2\phi^2 \quad . \tag{24}$$

Frankel and Acrivos [235], instead, related the viscous dissipation of energy in highly concentrated suspensions to the flow of a fluid within the narrow gaps between contiguous particles. As a result, the following expression have been obtained:

$$\mu_r = \frac{9}{8} \left[\frac{(\phi/\phi_m)^{\frac{1}{3}}}{1 - (\phi/\phi_m)^{\frac{1}{3}}} \right] \quad , \tag{25}$$

where ϕ_m is the maximum attainable concentration, as experimentally determined. Graham [238] improved the work of Frankel and Acrivos by means of a cell theory approach. The obtained model considers two contributions to the energy dissipation rate in a fluid cell, namely a contribute due to neighbor particle interactions and a contribute due to the flow through the cell and around the reference sphere. These considerations lead to:

$$\mu_r = 1 + 2.5\phi + 4.5 \left[\frac{1}{(\frac{h}{d_p})(2 + \frac{h}{d_p})(1 + \frac{h}{d_p})^2} \right] \quad , \tag{26}$$

where h is the envelope interparticle distance and d_p the particle diameter.

Finally, theoretical models of nanofluid viscosity may also account for particle aggregation [201, 236, 240].

26

5.2. Density

The effective nanofluid density (ρ_{nf}) is usually evaluated by a mixing rule [69, 195]:

$$\rho_{nf} = \frac{m_{nf}}{V_{nf}} = \frac{\rho_{bf}V_{bf} + \rho_p V_p}{V_{bf} + V_p} = (1 - \phi)\rho_{bf} + \phi\rho_p \quad, \tag{27}$$

where m_{nf} is the nanofluid mass, V_{nf} the nanofluid volume, V_{bf} the base fluid volume, V_p the particle volume, ρ_{bf} the base fluid density and ρ_p the particle density. Pak et al. [69] and Ho et al. [195] noticed a good agreement between this relation and their experimental tests on alumina-water nanofluids.

The effect of temperature on nanofluid density is not considered in Eq. (27). Accurate fittings of experimental measures of ρ_{bf} at different temperatures [135, 165, 241, 242] are usually obtained by [243]:

$$\rho_{bf} = \frac{a_0 + a_1 T + a_2 T^2 + a_3 T^3 + a_4 T^4 + a_5 T^5}{1 + a_6 T} \quad, \tag{28}$$

where T is the temperature (°C) and a_0 to a_6 are coefficients experimentally evaluated for the intended base fluid [242, 243]. Considering Eq. (28) and Eq. (27), Servati et al. [242] proposed a correlation for Al_2O_3-water nanofluids:

$$\rho_{nf} = \left(\frac{999.84 + 18.23T - 6.5 \times 10^{-3}T^2 - 5.4 \times 10^{-5}T^3}{0.0182T + 1} \right)$$
$$\times (1 - 1.1611\phi + 0.1611\phi^2) + \rho_p\phi(1 - 0.1611\phi) \quad, \tag{29}$$

in good agreement with experiments [195].

Also starting from the experimental results by Ho and colleagues [195], Khanafer and Vafai [165] presented a correlation between temperature and density of alumina-water nanofluids:

$$\rho_{nf} = (1001.064 + 2738.6191\phi - 0.2095T) \quad, \tag{30}$$

which is valid for $0 \leq \phi \leq 0.04$ and $5°C \leq T \leq 40°C$.

Finally, Vajjha et al. [241] measured the density of nanofluids containing alumina, antimony-tin oxide or zinc oxide nanoparticles suspended in a 60:40 (by weight) EG-water base fluid. To model the dependence of nanofluid density on temperature, Vajjha et al. took advantage of Eq. (27), assumed a constant value for ρ_p and considered:

$$\rho_{bf} = AT^2 + BT + C \quad , \tag{31}$$

where $A = -2.43 \times 10^{-6} \ g/cm^3 \cdot K^2$, $B = 9.6216 \times 10^{-4} \ g/cm^3 \cdot K$ and $C = 1.0099261 \ g/cm^3$.

Extended reviews regarding typical nanofluids densities can be found in references [69, 192, 195, 241].

6. Nanofluids in automotive cooling systems

Some peculiar characteristics are required for coolants in automotive applications. Regarding the thermo-physical properties, a coolant should possess high thermal conductivity, specific heat capacity and boiling point, as well as low viscosity and freezing point. In addition, it should be non-toxic and chemically inert, and it should not cause corrosion of the cooling system. Commercially available coolants for automobiles are usually characterized by a 50:50 (by mass) mixture of ethylene glycol and water. Freezing and boiling points of this mixture are -34 °C and 107 °C, respectively [244]. However, typical engine coolants have low thermal conductivity, namely: 0.613 W/mK and 0.253 W/mK for water and EG at 27°C, respectively (Table 2).

To enhance the heat transfer performance of cooling systems, it would be appropriate to use coolants with higher thermal conductivity. To this purpose, nanofluids can be an excellent alternative to traditional engine

coolants, as evident from the typical thermal conductivity values in Table 3. On the other hand, regardless of the enhancement in thermal conductivity, viscosity and specific heat capacity may cast doubt on the application of nanofluids as coolants for automotive engines. Therefore, a critical investigation on the overall properties of nanofluids and their influence on the performance of the cooling circuit is necessary.

A brief study of the engine cooling circuit is performed in this section, followed by the evaluation of thermal performance and efficiency of prototype cooling systems running with nanofluids.

6.1. Engine cooling circuit

A typical engine cooling system consists of radiator, fan, water pump, coolant reservoir, thermostat and the necessary plumbing for both radiator and heater core. During the warming-up process, once the engine is started, the coolant is pumped from the lower radiator tank to the engine block, where the coolant is heated by engine cylinders. Thermostat does not open until the coolant reaches the operating temperature. The state at which coolant has reaches the operating temperature is referred to as fully warmed-up condition. Then, heat energy is dissipated in the radiator, where heat is transferred to air flowing through the space between flat tubes and fins [25]. Usual temperature for the coolant at operating conditions is about 90 °C. The fan increases the heat transfer rate in the radiator in case of overheating. Moreover, the thermal energy accumulated in the coolant can be also used to heat up the cabin, thanks to an additional heater core.

It is highly beneficial to reduce warming-up time, as CO and HC emissions are much larger than in the fully warmed-up state (about 90% of HC emissions are emitted in the first 20 seconds) [26]. Nanofluids may represent

a way to decrease warming-up time. Let us consider an alumina-(W+EG) nanofluid: the effective specific heat capacity of the suspension is lower than the base fluid, while the density is higher. Hence, a lower volumetric heat capacity of nanofluid respect to base fluid one means a faster warm-up phase, leading to better combustion efficiency as well as reduced CO and HC emissions.

The ϵ-NTU method is usually adopted to determine heat transfer rate and outlet temperature of coolants flowing through heat exchangers. Here, the typical design of automotive radiators is illustrated for both air and coolant sides, in order to highlight the possible effects of nanofluid coolants on thermal control systems in the automotive field.

The mass flow rate of air through the radiator ($\dot{m}_a$) can be evaluated as:

$$\dot{m}_a = \rho_a A_{c,a} u_a \quad , \tag{32}$$

where ρ_a is the air density, $A_{c,a}$ the free flow area in the air side of radiator and u_a the air velocity. The convective heat transfer coefficient of air side (h_a) is instead evaluated as:

$$h_a = \frac{j_a \rho_a u_a c_{p,a}}{Pr^{2/3}} \quad , \tag{33}$$

where j_a is the Colburn factor, $c_{p,a}$ the specific heat capacity of air and Pr the Prandtl number.

The efficiency of the fins in the radiator (η_{fin}) can be calculated as:

$$\eta_{fin} = \frac{\tanh(mL_{fin})}{mL_{fin}} \quad , \tag{34}$$

where L_{fin} is the fin length and

$$m = \sqrt{\frac{2h_a}{k_{fin}t}} \quad , \tag{35}$$

30

being k_{fin} and t the thermal conductivity and the thickness of fins, respectively. Note that, low fin length or thermal conductivity will result in lower fin efficiency. To account for the overall heat transfer efficiency of the radiator on the air side, the total surface effectiveness (η_0) is defined as [2, 245]:

$$\eta_0 = 1 - (1 - \eta_{fin})A_{ft} \quad , \tag{36}$$

where A_{ft} is the ratio between fin area (A_{fin}) and total heat transfer surface (A).

Analogously, the mass flow rate of coolant ($\dot{m}_{nf}$) can be calculated as:

$$\dot{m}_{nf} = \rho_{nf} A_{c,nf} u_{nf} \quad , \tag{37}$$

where $A_{c,nf}$ is the free flow area in the coolant side of radiator and u_{nf} the nanofluid velocity. The convective heat transfer coefficient of coolant side (h_{nf}) can be evaluated as:

$$h_{nf} = \frac{Nu_{nf} k_{nf}}{D_{h,nf}} \quad , \tag{38}$$

where Nu_{nf} is the Nusselt number of the coolant (e.g. nanofluid), which depends on both characteristics of the system [9, 25, 246] and hydraulic diameter of the radiator tube ($D_{h,nf}$).

By neglecting the tube-wall thermal resistance, the overall heat transfer coefficient of the radiator (U_r) can be evaluated as:

$$\frac{1}{U_r} = \frac{1}{\eta_0 h_a} + \frac{1}{\frac{\alpha_{nf}}{\alpha_a} h_{nf}} \quad , \tag{39}$$

where α_a and α_{nf} are the ratio between total heat transfer area and total radiator volume (V_r) for air and nanofluid side, respectively.

The ϵ-NTU method can be then adopted, where the number of heat transfer units (NTU) is:

$$NTU = \frac{U_a \alpha_a V_r}{C_{min}} \quad , \tag{40}$$

31

being $C_{min}=\min(C_a, C_{nf})$ the minimum heat capacity rate between air and nanofluid. Heat capacity rate for air or nanofluid can be calculated as:

$$C = \dot{m}c_p. \tag{41}$$

The capacity ratio (C^*) between air and nanofluid is:

$$C^* = \frac{C_{min}}{C_{max}} \quad, \tag{42}$$

where $C_{max} = max(C_a , C_{nf})$. Subsequently, the heat exchanger effectiveness (ϵ) for a pure unmixed cross-flow configuration with an infinite number of passages is found as [245]:

$$\epsilon = 1 - \exp\left(\frac{1}{C^*}\right)(NTU)^{0.22}\left[\exp[-C^*(NTU)^{0.78}] - 1\right]. \tag{43}$$

The heat flux exchanged in the radiator $(\dot{Q})$ can be finally evaluated as:

$$\dot{Q} = \epsilon C_{min}\left(T_{nf,in} - T_{a,in}\right) \quad, \tag{44}$$

where $T_{nf,in}$ and $T_{a,in}$ are the inlet temperature of coolant and air, respectively.

The pressure drop experienced by the coolant in the radiator (ΔP_{nf}) can be estimated as:

$$\Delta P_{nf} = \frac{f_{nf}L_r\rho_{nf}u_{nf}^2}{2D_{h,nf}} \quad, \tag{45}$$

where f_{nf} is the friction factor of nanofluid coolant [9, 25] and L_r the radiator length. Eventually, the required pumping power (W) is:

$$W = \dot{V}_{nf}\Delta P_{nf} \quad, \tag{46}$$

where $\dot{V}_{nf}$ is the nanofluid volumetric flow rate.

6.2. Efficiency of nanofluid coolants

The heat transfer enhancement by nanofluid coolants is generally accompanied with the increase in pressure drop [247]. Hence, a compromise between the higher heat transfer and the associated higher pressure losses has to be considered by introducing performance indexes.

In a experimental study, Razi et al. [248] investigated the heat transfer and pressure drop characteristics of the flow of a nanofluid in a tube. To improve the heat transfer coefficient, they adopted nanofluid coolants (i.e. CuO-oil) and flattened tubes, instead of conventional base fluids and round tubes. Then, heat transfer coefficient and pressure drop were measured in a broad variety of configurations. To quantify the overall benefits of nanofluid coolants, they defined an efficiency coefficient as:

$$
\eta_I = \frac{\left(\dfrac{h^*}{h_{RT,bf}} \right)}{\left(\dfrac{\Delta P^*}{\Delta P_{RT,bf}} \right)} \quad . \tag{47}
$$

h^* and ΔP^* are heat transfer coefficient and pressure drop for the nanofluid configuration, whereas $h_{RT,bf}$ and $\Delta P_{RT,bf}$ refer to the flow of conventional oil coolant inside a round tube. Based on Eq. (47), a performance index (η_I) greater than 1 implies that the advantages due to heat transfer enhancement by either nanofluid or flattened tubes overcome the increase in pressure drop. In particular, Razi et al. [248] found that a maximum value for the performance index (i.e. η_I=1.43) was observed for the nanofluid flow within flattened tubes with internal height of 7.5 mm and *Re=23.5*. Specifically, they found that:

$$
\eta_{I,nf,FT} > \eta_{I,nf,RT} > \eta_{I,bf,RT} \quad ,
$$

which indicates that using nanofluids within flat tubes is an efficient strategy for enhancing overall performances of traditional heat exchangers.

Results from Razi et al. [248] experiments also showed that the Nusselt number for the CuO-oil nanofluid (¡2 wt% particle concentration) in the fully developed hydrodynamic laminar flow regime ($Re < 120$) and within flattened tubes ($1 < D/D_h < 1.3$) can be interpolated by:

$$Nu_{nf} = 0.0812 Re_{nf}^{0.587} Pr_{nf}^{0.389} \left(\frac{D}{D_h} \right)^{1.297} (1 + \phi)^{56.147} \quad , \qquad (48)$$

where Re_{nf} is the nanofluid Reynolds number, Pr_{nf} the nanofluid Prandtl number, D the round tube diameter, and D_h the flattened tube hydraulic diameter. Hence, the heat transfer coefficient was finally calculated as:

$$h_{nf} = \frac{Nu_{nf} \times k_{nf}}{D^*} \quad , \qquad (49)$$

where D^* stands for either D or D_h.

On the other hand, Ray at al. [25] suggested to calculate Nu of the base fluid inside flat tubes with the Bejan and Gnielinski correlations [249, 250]:

$$Nu_{bf} = 0.012(Re_{bf}^{0.87} - 280)Pr_{bf}^{0.4} \quad , \qquad (50)$$

with $1.5 \leq Pr_{bf} \leq 500$ and $3 \times 10^3 \leq Re_{bf} \leq 10^6$. Instead, they proposed an expression derived by Vajjha et al. [251] to compute Nu of the nanofluid coolant:

$$Nu_{nf} = 0.0222(Re_{nf}^{0.8} - 60)Pr_{nf}^{0.4}(1 + 0.32178\phi^{0.64788}) \quad , \qquad (51)$$

with $17.6 \leq Pr_{nf} \leq 38.6$ and $3000 \leq Re_{nf} \leq 16000$.

Ferrouillat and co-workers [252] carried out an experimental work on the influence of nanoparticle shape on the overall energy performances of nanofluids for cooling applications. They measured the pressure drops and

heat transfer coefficients of water-based SiO_2 and ZnO nanofluids, which were flowing within a horizontal tube at different inlet temperatures and flow rates. Results indicated a small improvement in the Nusselt number with nanofluid coolants. Moreover, they defined a second efficiency coefficient (η_{II}) to characterize the performance of fluid coolants. This coefficient compares the heat flux transferred ($\dot{Q}$) and the required pumping power (W) for nanofluid and conventional coolants, namely:

$$\eta_{II} = \frac{\dot{Q}_{nf}/W_{nf}}{\dot{Q}_{bf}/W_{bf}} \quad , \tag{52}$$

where $\dot{Q}$ and W are derived from Eqs. (44) and (46), respectively. Results showed that $\eta_{II} > 1$, i.e. nanofluid coolants with overall energy performances higher than water, only in case of suspended ZnO nanoparticles with shape factor greater than 3.

6.3. Nanofluid coolants for automotive applications

Taking advantage from the relations between nanofluid characteristics and resulting thermo-physical properties discussed in previous sections, it may be possible to rational design nanofluids with large heat transfer rate while keeping the required pumping power as low as possible. In the following, some of the research works on the application of nanofluids in automotive radiators are reviewed.

In a numerical study, Bai et al. [253] assessed the heat transfer capability of Cu, Al, Al_2O_3 and TiO_2 water-based nanofluids in an engine cooling system ($\dot{V}$=155 l/min). According to their results, the Cu-water nanofluid (ϕ=5%) showed the largest heat transfer coefficient (h_{nf}=6251.77 W/m^{2}K), namely 46% more than pure water (h_{bf}=4282.84 W/m^{2}K). Hence, the average heat dissipation potential of the nanofluid for a single cylinder

($\dot{Q}$=2937.2 W) was 43.9% higher than in case of pure water. The pumping power, instead, increased by 6% because of the higher pressure drop for Cu-water nanofluid (ΔP_{nf}=24 kpa) as compared to water coolant (ΔP_{bf}=17 kpa).

Vajjha et al. [168] performed a numerical study for assessing both fluid dynamics and heat transfer performance of Al_2O_3 and CuO nanofluids in the flat tubes of a radiator. The nanofluid flow was under laminar regime, with Reynolds numbers spanning from 100 to 2000. Results allowed to establish two new correlations for the Nusselt number in the entrance region:

$$Nu = 1.9421 \left(RePr \frac{D_h}{Z} \right)^{0.3} \quad , \tag{53}$$

valid for

$$\left(RePr \frac{D_h}{Z} \right) \geq 33.33 \quad ,$$

and

$$Nu = 6.1 + 0.003675 \left(RePr \frac{D_h}{Z} \right) \quad , \tag{54}$$

valid for

$$\left(RePr \frac{D_h}{Z} \right) < 33.33 \quad ,$$

where Z is the axial distance from the inlet. This analysis showed a heat transfer increase with both Reynolds number and particle concentration. Based on their numerical results, heat transfer coefficients of Al_2O_3 ($\phi = 10\%$) and CuO ($\phi = 6\%$) nanofluids at $Re=2000$ were 94% and 89% higher than the base fluid, respectively. Furthermore, they observed that, for a constant inlet velocity, the friction factor along the duct increased with the particle volume concentration. On the other hand, the same heat transfer co-efficient could be achieved by a lower volumetric flow rate of nanofluids than conventional coolants, and thus less pumping power was required. In fact,

in the laminar flow regime and for the same amount of heat transferred, the required pumping power for Al_2O_3 (ϕ=10%) and CuO nanofluids (ϕ=6%) was 82% and 77% lower than the one required for the base fluid, respectively. Hence, the performance index (η_I) was 1.30 and 1.14 for the alumina and copper oxide nanofluids, respectively (Re=2000 and h=910 W/m^{2}K). These results are a preliminary proof of the potential of using nanofluid coolants in car radiators.

Peyghambarzadeh et al. [254] experimentally analyzed the heat transfer performance of a nanofluid in a car radiator with louvered fins and flat tubes. They carried out a systematic experimental evaluation of the thermal transfer efficiency for pure water, pure ethylene glycol (EG) as well as water-EG mixtures. Subsequently, Al_2O_3 nanoparticles were added in these base fluids, and the resulting performance variations recorded (particle volume concentration spanning from 0.1 to 1%; flow rate from 1 to 6 l/min). The Nusselt number in the nanofluid cases increased up to 40% with both volume concentration of particles and Reynolds number. Furthermore, Peyghambarzadeh and colleagues found that by increasing the nanofluid inlet temperature ($T_{nf,in}$) from 35°C to 50°C, the Nusselt number of water-based nanofluids increased by 16%. Instead, for the EG-based nanofluids, an enhancement of 7% was evident by increasing the $T_{nf,in}$ from 45°C to 60°C. Eventually, they also studied the performance of EG- and water-based alumina nanofluids by varying the concentration of EG (from 5% to 20%), the Al_2O_3 volume concentration (from 0 to 0.3%) and the flow rate. Results showed that by increasing the EG percentage in water, the Nusselt number decreased, since water has better thermal properties than EG. Moreover, by increasing the particle volume fraction and flow rate, the Nusselt number significantly increased.

Hussein et al. [24] performed an experimental and computational study of the heat transfer performances of a car radiator running with SiO_2-water nanofluid under laminar flow. They set up a test rig to measure heat transfer coefficient and friction factor of the nanofluid coolant (Fig. 7). Hussein and colleagues observed that the friction factor of nanofluid was inversely proportional to the flow rate, whereas directly proportional to the particle volume fraction. The decrease in friction factor by increasing the Reynolds number, instead, was in accordance with the Darcy-Weisbach equation for laminar flow conditions. Moreover, the Nusselt number increased with flow rate, nanofluid volume concentration and inlet temperature. Particularly, the increase of inlet temperature ($T_{nf,in}$) from 60 °C to 80 °C led to Nusselt number increase from 17.8 to 25. Therefore, SiO_2-water nanofluids with low volume concentration of nanoparticles was proven to be able to enhance heat transfer rate up to 50% compared to pure water.

Leong et al. [9] investigated the heat transfer characteristics of EG-based copper nanofluids in a car radiator. They observed that, at a fixed air side Reynolds number (i.e. *Re=4000*), the overall heat transfer coefficient on the air side increased with both Reynolds number of coolant and volume concentration of particles (Fig. 8). Hence, they concluded that the use of nanofluids may allow to reduce the heat transfer area of automotive radiators. A reduction of 18.7% was estimated for the air frontal area at Re_{air}=6000 and $Re_{coolant}$=5000 when the base fluid was replaced by a 2% copper nanoparticle suspension. Furthermore, Leong et al. noticed an increase in coolant pressure drop with the addition of copper nanoparticles. Results revealed a pressure drop of 110.97 kPa by adding 2% copper particles, instead of 98.93 kPa in case of pure water. Hence, an additional pumping power of 12.13% was required with nanofluid coolants at 0.2 m³/s volumetric flow rate. Con-
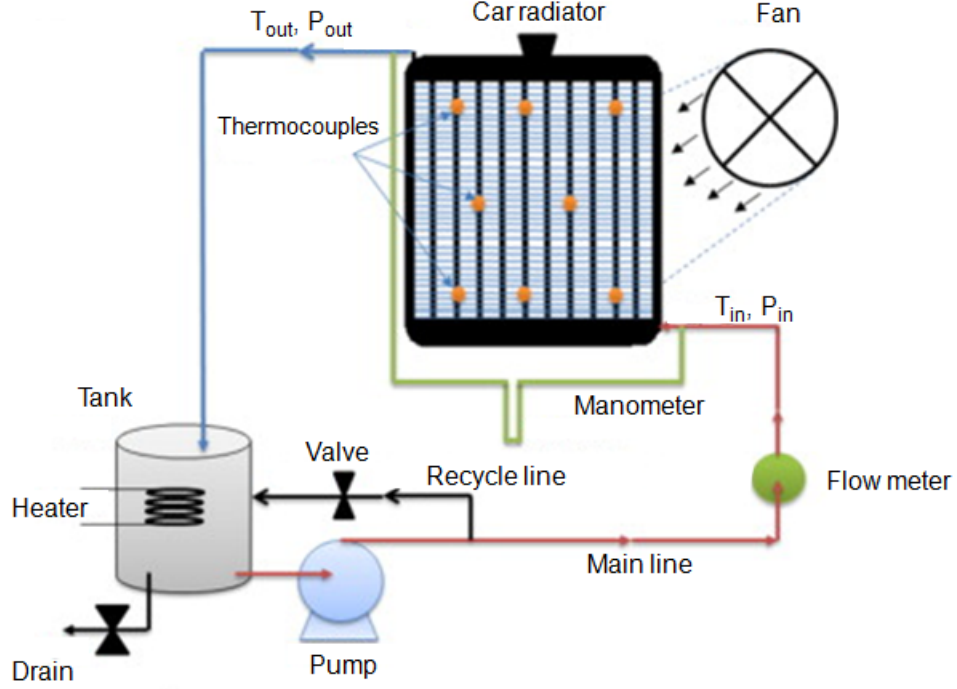
Figure 7: Schematic diagram of an experimental test rig for nanofluid coolants. The test rig includes an automotive radiator, 10 thermocouples type T to measure temperature, tubes (0.5 in), a fan, a manometer tube with mercury, a flow meter (0÷70 LPM), two valves, a centrifugal pump (0.5 hp and 3 m head), a reservoir plastic tank, a DC power supply and an electrical heater. Figure adopted from reference [24].

sidering the data available in this study at Re_{air}=4000 and $Re_{coolant}$=7000, the energy efficiency of the 2% Cu-EG nanofluid coolant $\eta_I \approx 1$ in Eq. (47) was found, meaning that no significant overall performance improvement in using nanofluid rather than traditional coolants was noticed.

Huminic et al. [255] employed a numerical approach to assess the heat transfer characteristics of a CuO-EG nanofluid flowing in flattened tubes of automobile radiator under a laminar flow regime. They evaluated the effects of volume concentration (0 to 4%) and Reynolds number (0 to 125)
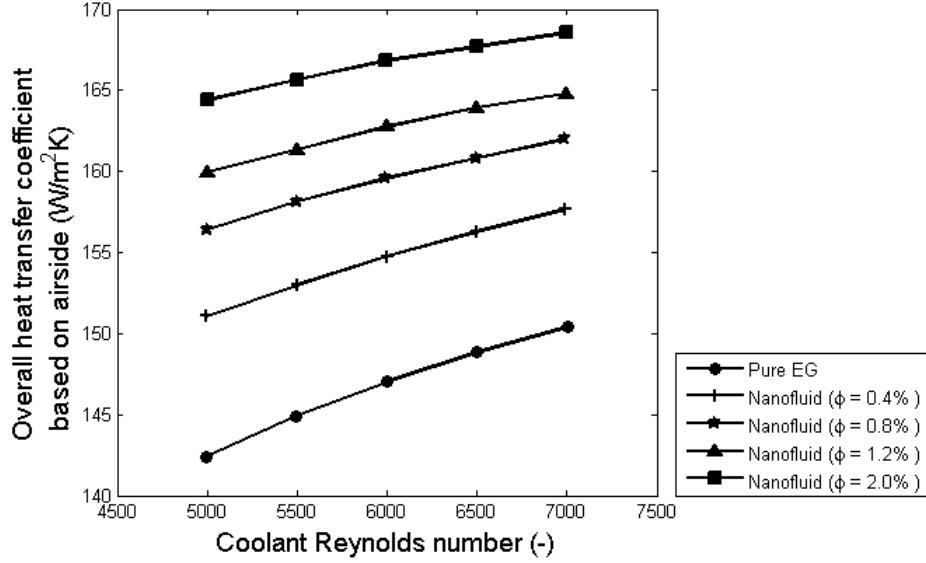
Figure 8: Air side overall heat transfer coefficient of Cu-EG nanofluids at different Reynolds numbers and particle volume fraction. Figure reproduced based on reference [9].

on the heat transfer performance of the car radiator. Results showed a Nu increase with both volume fraction and Reynolds number. For instance, a 19% enhancement in the heat transfer coefficient at Re=10 and $\phi = 4\%$ was reported. Furthermore, by comparing flattened, elliptical and circular tubes, they realized that flattened tubes can substantially increase (up to 82% enhancement, Fig.9) heat transfer coefficient.

In summary, thermo-physical properties of nanofluids (ρ, μ, c_p, k) have been observed to change with nanofluid characteristics (e.g. particle volume fraction, particle shape and size, particle and base fluid material, temperature). The variation of the nanofluid characteristics, on one hand, leads to changes in the dimensionless numbers (i.e. Re and Pr) required for evaluating the heat transfer coefficient of cooling system. On the other hand,
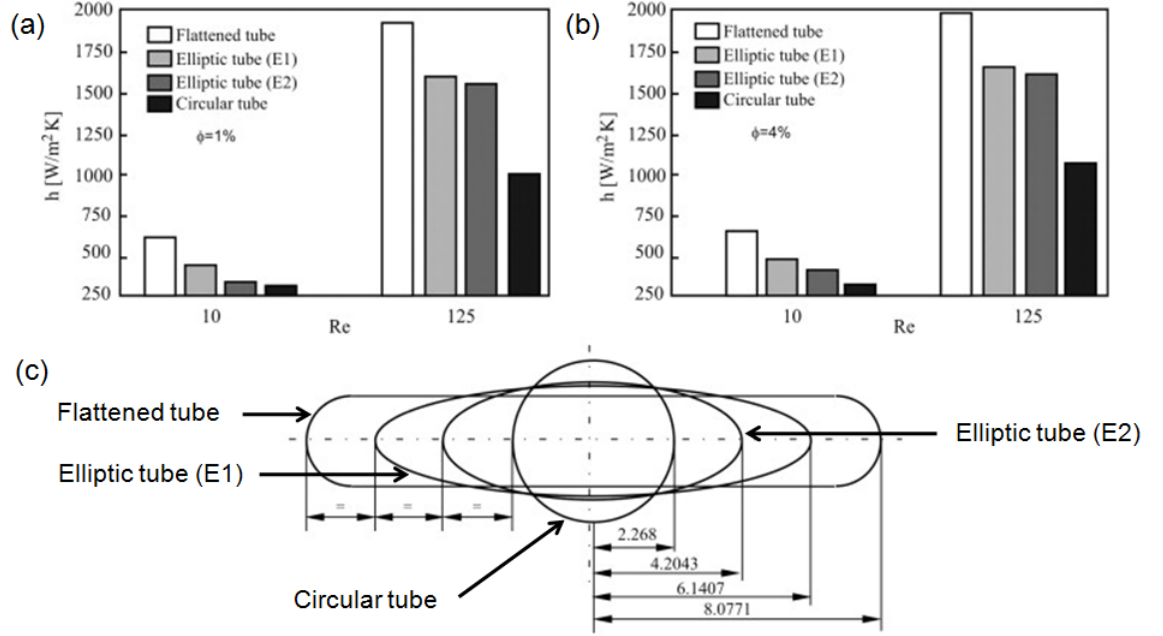
Figure 9: Heat transfer coefficient of a radiator tube. (a) Influence of Re and tube cross section on h_{nf} at $\phi = 1\%$ (b) Influence of Re and tube cross section on h_{nf} at $\phi = 4\%$ (c) Considered tube cross sections. Figure adopted from reference [255].

the variation in Re leads to changes in f, ΔP and hence the required pumping power, which is generally higher for systems working with nanofluid coolants. Hence, one should systematically assess the overall influence of these parameters on the energy performance of the system by means of the efficiency indexes in Eqs. (47) and (52).

7. Challenges and perspectives

In this section the challenges and barriers to a wider industrial application of nanofluids are reviewed. Moreover, perspectives for further development of nanofluid research are indicated, with the aim to resolve the

inconsistencies reported in the current literature.

First, properties of nanofluids cannot be predicted by classical continuum models and, currently, there is no general theoretical model which can forecast their heat and mass transfer characteristics. Particularly, several mechanisms have been proposed to explain the enhanced heat conduction of nanofluids, such as nanolayer, interfacial thermal resistance, aggregation and percolation phenomena. However, the interplay between these mechanisms and the resulting effect on thermo-physical properties of nanofluids have not yet been systematically understood. Second, evidences from different experimental studies are not consistent, and usually not even well understood. Third, large-scale and low-cost production of stable nanoparticle suspensions has not yet been achieved.

Various geometrical, chemical and physical parameters can affect the nanofluid stability, as well as its heat transfer and rheological properties. Hence, a possible explanation for the existence of contradictory experimental results could be the different production techniques and experimental protocols adopted for synthesizing and testing nanofluids. These inconsistencies strongly influence the nanofluid properties.

To address these controversies and allow a more systematic study of the underlying phenomena, experimental studies on nanofluids should always detail: (1) the synthesis method adopted for preparing the nanofluid; (2) the nanoparticle characteristics (core and coating material, particle shape) as well as the type of surfactant introduced (if any); (3) the concentration of nanoparticles and surfactants; (4) the size distribution of nanoparticles; (5) the base fluid properties; (6) the pH and zeta-potential of the suspension during different stages of the experiment; (7) the concentration of additives used for adjusting the pH of the suspension (if any); (8) the presence of

particle clusters as well as the average aggregates size; (9) the time elapsed after the nanofluid synthesis; (10) the temperature at which experiments are conducted; (11) the measurement techniques adopted and any other helpful data that can provide the reader with a complete understanding of the conducted experiment.

On the other hand, results of experimental studies on nanofluids should be properly analyzed. It is generally accepted that by suspending nanoparticles in a base fluid, effective thermal conductivity, viscosity and density increase, while heat capacity decreases. Hence, the nanofluid performance cannot be judged by merely evaluating the resulting heat transfer coefficient (h_{nf}), while an overall analysis should be considered. In particular, a meaningful quantity to assess the technical feasibility of nanofluids as automotive coolants is the efficiency index, which compares the beneficial enhancement in thermal conductivity with the general viscosity (i.e. pumping power) increase. Similarly, also the Prandtl number is a good reference for evaluating the balance between thermal conductivity and viscosity enhancements in nanofluids. As shown in Tables 4 and 5, several studies on nanofluids reported efficiencies and Prandtl numbers larger than one, therefore demonstrating that nanofluids are energy efficient alternatives to traditional automotive coolants. In addition, the working conditions of the nanofluid in each specific application should be critically investigated. Considering typical automotive cooling system, the operating conditions of the engine and thus of the cooling circuit, such as temperature, flow regime and the suitable coolant pH, should be taken into account. Engine coolants usually operate in the temperature range between 50°C - 110°C [25]. In that temperature interval, nanofluid thermal conductivity tends to increase with temperature, while viscosity decreases. However, there exists a critical temperature be-

43

yond which a irreversible degradation of nanofluid properties may occur.

Table 4: Energy efficiency of nanofluids for automotive cooling applications.

NP material	Base fluid	$\phi(\%)$	T (°C)	η_I	η_{II}	Reference
Cu	W	5	70	1.034	1.019	[253]
CuO	60:40 EG/W	6	90	1.141	-	[168]
Al$_2$O$_3$	60:40 EG/W	10	90	1.304	-	[168]
CuO	Oil	2(wt%)	-	1.43	-	[248]
ZnO	W	0.93	15-90	-	1.097	[252]
SiO$_2$	W	2.28	15-90	-	0.930	[252]

Another important factor influencing the performances of nanofluid coolants is the flow regime, which can drastically change their thermal and rheological properties. Moreover, the pH of coolant should be carefully designed, since it has direct impact on the corrosion of radiator and tubes in automotive cooling systems [244]: for most of the cars, pH should be maintained in the range $7.5 \div 10.5$ [257]. Hence, the pH of nanofluids can be adjusted towards these practical range, which also induces further thermal conductivity enhancement (Table 6). Considering the zeta-potential and the pH range in Table 6, one can understand that those thermal conductivity enhancements have been reported far from the isoelectric points of Al$_2$O$_3$-water and Cu-water suspensions. For this reason, the thermal conductivity enhancement and viscosity variation in nanofluid coolants should be generally convenient within the practical pH range for automotive applications.

Finally, the development of large-scale production techniques is also required to obtain nanofluids with good stability, repeatability and low production costs. Both the current single- and two-step techniques are fac-

Table 5: Prandtl number enhancement in nanofluids for automotive cooling applications.

NP material	Base fluid	$\phi(\%)$	T (°C)	Pr_{nf}/Pr_{bf}	References
Al_2O_3	60:40 EG/W	5	25	1.475	[25]
CuO	60:40 EG/W	5	25	2.064	[25]
SiO_2	60:40 EG/W	5	25	1.231	[25]
Cu	W	2	70	0.914	[253]
Al	W	2	70	0.916	[253]
TiO_2	W	2	70	0.939	[253]
SiO_2	W	2	50	0.867	[24],[256]
Al_2O_3	W	2	50	1.605	[24],[256]
TiO_2	W	2	50	1.379	[24],[256]
Al_2O_3	W	1	77	0.953	[26]

Table 6: Nanofluid properties at practical pH ranges for automotive applications.

Nanofluid	pH range	Zeta potential (mV)	Weight fraction	k_{nf}/k_{bf}	Temperature (°C)	surfactant	References
Cu-Water	8 to 11	-44 to -40	0.05 wt%	9%	25	SDBS	[77, 118]
Al_2O_3-Water	8 to 11	-40 to -33	0.05 (wt%)	8 %	25	SDBS	[118]
ZrO_2-Water	8 to 10	-12 to -25	3 (wt%)	5 to 30 %	25	-	[136]
TiO_2-Water	-	-47.9	0.1 (wt%)	10 %	-	SDS	[258]

ing difficulties that should be addressed to scale up nanofluids synthesis. As regards two-step methods, the challenge is to overcome large van der Waals agglomeration of nanoparticles, for example by means of proper surface treatment or particle coating. The current drawbacks of single-step techniques, instead, are the higher cost of synthesis, as well as the limited control over nanoparticle size distribution.

8. Conclusions

Thanks to their enhanced thermo-physical properties, nanofluids are showing great potential in energy, mechanical and biomedical fields. Mainly, the high thermal conductivity of nanofluids can guarantee extremely efficient heat exchange in automotive cooling applications. However, a more rational design of these nanoparticle suspensions requires a better understanding of their nanoscale characteristics and resulting macroscale properties. This review supplies an in-depth description of the state of the art in nanofluids, from synthesis to thermo-physical properties, in the context of automotive applications.

Special attention is paid to the critical dependency of thermal conductivity (k) on nanoscale mechanisms in nanofluids. In detail, k is strongly enhanced by a highly conductive liquid nanolayer around the surface of the particles. Moreover, particle-fluid heat conduction is also affected by the interfacial thermal resistance, which is not negligible at this scale. Brownian motion also plays a crucial role in nanofluid properties: although particle diffusion is extremely slow compared to heat diffusivity, Brownian motion affects the agglomeration of particles and thus the formation of thermal percolating paths. Unfortunately, significant aggregation into sparse but large

46

clusters increases both thermal transport and fluid viscosity. Hence, future researches should investigate the optimal nanofluid aggregate morphologies leading to the best combination of thermal conductivity, viscosity and stability.

This review presents several theoretical and empirical models describing nanofluid thermal conductivity, viscosity, specific heat capacity and density. Specifically, a strong sensitivity of nanofluid properties to their design characteristics (i.e. particle material, shape, size and volume concentration, base fluid pH and surfactant concentration) is noticeable in the available literature. This extremely pronounced sensitivity could be identified as the main reason for some contradictory results in the large amount of models and the experimental evidences in the literature.

The ultimate purpose of this review is highlighting the advantages of nanofluids as coolants for automotive heat exchangers, and a number of guidelines have been suggested for their rational design and usage. However, although thousands of studies have addressed a more mechanistic understanding of nanofluid properties, comprehensive models relating nanoscale effects to their macroscopic behavior are still missing. Such multiscale models would facilitate and systematize the translation of nanofluid technology from small-scale experiments to large scale industrial production and commercialization.

Competing interests

The authors declare that they have no competing interests.

Acknowledgments

Nomenclature

ΔP Pressure drop (Pa)

$\dot{Q}$ Heat transfer rate (W)

$\dot{V}$ Volumetric flow rate (m^3/s)

$\dot{m}$ Mass flow rate (kg/s)

AR Aspect ratio (–)

D_h Hydraulic diameter (m)

D_p Brownian diffusion coefficient (m^2/s)

E Interaction energy (J)

G_k Thermal boundary conductance (W/ m^2 K)

L_r Radiator length (m)

Nu Nusselt number (–)

Pr Prandtl number (–)

R_k Kapitza resistance (m² K/W)

Re Reynolds number (–)

T Temperature (°C)

U_r Overall heat transfer coefficient of the radiator (W/m² K)

V_r Total radiator volume (m³)

V Volume (m³)

W Pumping power (W)

c_p Specific heat capacity (J/kg K)

d_{bf} Base fluid molecule diameter (m)

d_p Particle diameter (m)

f Friction factor (–)

h Heat transfer coefficient (W/m² K)

k_B Boltzman constant (J/K)

k_a Thermal conductivity of aggregates (W/m K)

k Thermal conductivity (W/m K)

l_k Kapitza length (m)

n Shape factor (–)

q Heat flux per unit area (W/m²)

r_p Particle radius (m)

u Velocity (m/s)

v Phonon velocity (m/s)

Greek Symbols

β Thermal expansion coefficient (K^{-1})

δ Nanolayer thickness (m)

ϵ Heat exchanger effectiveness (–)

η Efficiency (–)

η_0 Total surface effectiveness (–)

μ Viscosity (Pa·s)

ϕ Volume fraction (–)

ϕ_a Volume fraction of aggregates (–)

ψ Sphericity (–)

ρ Density (kg/m^3)

τ_D Time scale of particle motion (s)

τ_H Time scale of heat diffusion (s)

Subscripts

bf Base fluid

$elec$ Electrostatic

fr Freezing point

FT Flat tube

in Tube inlet

kf Krafft point

nf nanofluid

pe Equivalent particle

p particle

RT Round tube

r ratio

sfc Surfactant

tot Total

vw van der Waals

Chemical formulas

CTAB Cetyl trimethyl ammonium bromide

SDBS Sodium dodecyl benzene sulfonate

SDS   Sodium dodecyl sulfate

Abbreviations

BG   Bruggeman

CMC   Critical micelle concentration

CNT   Carbon nanotube

DLVO Derjaguin, Landau, Verwey, and Overbeek

DSC   Differential scanning calorimetry

EDL   Electric double layer

EG   Ethylene glycol

EO   Engine oil

HC   Hamilton-Crosser

IEP   Isoelectric point

MG   Maxwell-Garnett

MWCNT Multi-walled carbon nanotube

NTU   Number of heat transfer units

OA   Oleic Acid

SSA   Specific surface area

References

[1] D. Wen, G. Lin, S. Vafaei, K. Zhang, Review of nanofluids for heat transfer applications, Particuology 7 (2) (2009) 141–150.

[2] R. L. Webb, N.-H. Kim, Principl of enhanced heat transfer, Taylor Francis: New York, NY, USA .

[3] S. Liu, M. Sakr, A comprehensive review on passive heat transfer enhancements in pipe exchangers, Renewable and Sustainable Energy Reviews 19 (2013) 64–81.

[4] F. Cola, M. De Gennaro, D. Perocchio, E. Canuto, S. Daniele, P. Napoli, G. T. Rivalta, E. Chiavazzo, M. Fasano, P. Asinari, Integrated receivers with bottom subcooling for automotive air conditioning: detailed experimental study of their filling capacity, International Journal of Refrigeration .

[5] L. Ventola, M. Dialameh, M. Fasano, E. Chiavazzo, P. Asinari, Convective heat transfer enhancement by diamond shaped micro-protruded patterns for heat sinks: Thermal fluid dynamic investigation and novel optimization methodology, Applied Thermal Engineering 93 (2016) 1254–1263.

[6] E. Chiavazzo, L. Ventola, F. Calignano, D. Manfredi, P. Asinari, A sensor for direct measurement of small convective heat fluxes: Validation and application to micro-structured surfaces, Experimental Thermal and Fluids Science 55 (2014) 42–53.

[7] L. Ventola, F. Robotti, M. Dialameh, F. Calignano, D. Manfredi, E. Chiavazzo, P. Asinari, Rough surfaces with enhanced heat transfer for electronics cooling by direct metal laser sintering, International Journal of Heat and Mass Transfer 75 (2014) 58–74.

[8] D. P. Kulkarni, R. S. Vajjha, D. K. Das, D. Oliva, Application of aluminum oxide nanofluids in diesel electric generator as jacket water coolant, Applied Thermal Engineering 28 (1415) (2008) 1774 – 1781.

[9] K. Leong, R. Saidur, S. Kazi, A. Mamun, Performance investigation of an automotive car radiator operated with nanofluid-based coolants (nanofluid as a coolant in a radiator), Applied Thermal Engineering 30 (1718) (2010) 2685 – 2692.

[10] R. D. Hercamp, R. D. Hudgens, G. E. Coughenour, Aqueous propylene glycol coolant for heavy duty engines, Tech. Rep., SAE Technical Paper, 1990.

[11] R. J. Boyle, I. Finlay, T. Biddulph, R. Marshall, Heat transfer to non-aqueous engine coolants, Tech. Rep., SAE Technical Paper, 1991.

[12] W. J. Kilmartin, D. C. Dehm, Aqueous Propylene Glycol Engine Coolant for Automotive and Light Duty Applications, Tech. Rep., SAE Technical Paper, 1993.

[13] A. Zadrozny, Propylene Glycol Coolant: A Safer Alternative for Heavy Duty Vehicles, Tech. Rep., SAE Technical Paper, 1993.

[14] D. A. Washington, D. L. Miller, J.-P. Maes, P. Van de Ven, J. E. Orth, Long life performance of carboxylic acid based coolants, Tech. Rep., SAE Technical Paper, 1994.

[15] G. E. Coughenour, D. R. Goodman, A. J. Brunett, S. L. Ellis, High Temperature, High Load Performance of Propylene Glycol Engine Coolants in Modern Gasoline Engines, Tech. Rep., SAE Technical Paper, 1995.

[16] M. Gollin, E. V. McAssey, C. Stinson, Comparative performance of ethylene glycol/water and propylene glycol/water coolants in the con-

vective and forced flow boiling regimes, Tech. Rep., SAE Technical Paper, 1995.

[17] S. U. Choi, J. Eastman, Enhancing thermal conductivity of fluids with nanoparticles, Tech. Rep., Argonne National Lab., IL (United States), 1995.

[18] S. M. Vanaki, P. Ganesan, H. Mohammed, Numerical study of convective heat transfer of nanofluids: A review, Renewable and Sustainable Energy Reviews 54 (2016) 1212–1239.

[19] M. Chandrasekar, S. Suresh, A. C. Bose, Experimental studies on heat transfer and friction factor characteristics of Al_2O_3/water nanofluid in a circular pipe under laminar flow with wire coil inserts, Experimental Thermal and Fluid Science 34 (2) (2010) 122 – 130.

[20] F. He, D. Ewing, J. Finn, J. Wagner, L. Ma, Thermal Management of Vehicular Payloads Using Nanofluid Augmented Coolant Rail-Modeling and Analysis, Tech. Rep., SAE Technical Paper, 2013.

[21] R. Saidur, K. Leong, H. Mohammad, A review on applications and challenges of nanofluids, Renewable and Sustainable Energy Reviews 15 (3) (2011) 1646–1668.

[22] M. Corcione, M. Cianfrini, A. Quintino, Optimization of laminar pipe flow using nanoparticle liquid suspensions for cooling applications, Applied Thermal Engineering 50 (1) (2013) 857 – 867.

[23] S. Srivastava, N. S. Chauhan, Nanofluids: Effectual Analysis in Automotive Application, Tech. Rep., SAE Technical Paper, 2014.

[24] A. M. Hussein, R. Bakar, K. Kadirgama, Study of forced convection nanofluid heat transfer in the automotive cooling system, Case Studies in Thermal Engineering 2 (0) (2014) 50 – 61.

[25] D. R. Ray, D. K. Das, Superior Performance of Nanofluids in an Automotive Radiator, Journal of Thermal Science and Engineering Applications 6 (4) (2014) 041002.

[26] M. V. Millan, S. Samuel, Nanofluids and Thermal Management Strategy for Automotive Application, Tech. Rep., SAE Technical Paper, 2015.

[27] A. Amiri, M. Shanebedi, B. Chew, S. Kazi, K. Solangi, Toward improved engine performance with crumpled nitrogen-doped graphene based water-ethylene glycol coolant, Chemical Engineering Journal .

[28] T. Borbáth, D. Bica, I. Potencz, L. Vékás, I. Borbáth, T. Boros, Magnetic nanofluids and magnetic composite fluids in rotating seal systems, in: IOP Conference Series: Earth and Environmental Science, vol. 12, IOP Publishing, 012105, 2010.

[29] C. J. Choi, S. P. Jang, S. U. Choi, Electrokinetic effects of charged nanoparticles in microfluidic Couette flow, Journal of Colloid and Interface Science 363 (1) (2011) 59 – 63.

[30] K. Lee, Y. Hwang, S. Cheong, L. Kwon, S. Kim, J. Lee, Performance evaluation of nano-lubricants of fullerene nanoparticles in refrigeration mineral oil, Current Applied Physics 9 (2, Supplement) (2009) e128 – e131.

[31] A. Moradi, E. Sani, M. Simonetti, F. Francini, E. Chiavazzo, P. Asinari, Carbon-nanohorn based nanofluids for a direct absorption solar collector for civil application, Journal of Nanoscience and Nanotechnology 15 (5) (2015) 3488–3495.

[32] L. Zhang, Y. Ding, M. Povey, D. York, ZnO nanofluids-A potential antibacterial agent, Progress in Natural Science 18 (8) (2008) 939–944.

[33] J. Liu, J.-F. Yan, Z.-S. Deng, Nano-cryosurgery: a basic way to enhance freezing treatment of tumor, ASME 2007 International Mechanical Engineering Congress and Exposition (2007) 87–94.

[34] A. Gizzatov, J. Key, S. Aryal, J. Ananta, A. Cervadoro, A. L. Palange, M. Fasano, C. Stigliano, M. Zhong, D. Di Mascolo, et al., Hierarchically structured magnetic nanoconstructs with enhanced relaxivity and cooperative tumor accumulation, Advanced Functional Materials 24 (29) (2014) 4584–4594.

[35] A. Cervadoro, M. Cho, J. Key, C. Cooper, C. Stigliano, S. Aryal, A. Brazdeikis, J. F. Leary, P. Decuzzi, Synthesis of Multifunctional Magnetic NanoFlakes for Magnetic Resonance Imaging, Hyperthermia, and Targeting., ACS applied materials & interfaces 6 (15) (2014) 12939–12946.

[36] I. Global Industry Analysts, Automotive radiators: A global strategic business report, `http://www.strategyr.com/Automotive_Radiators_Market_Report.asp`, 2015.

[37] S. Choi, Enhancing thermal conductivity of fluids with nanoparticles, ASME-Publications-Fed 231 (1995) 99–106.

[38] P. Keblinski, S. Phillpot, S. Choi, J. Eastman, Mechanisms of heat flow in suspensions of nano-sized particles (nanofluids), International journal of heat and mass transfer 45 (4) (2002) 855–863.

[39] S. Murshed, K. Leong, C. Yang, Enhanced thermal conductivity of TiO_2water based nanofluids, International Journal of Thermal Sciences 44 (4) (2005) 367–373.

[40] J. Xu, K. Bandyopadhyay, D. Jung, Experimental investigation on the correlation between nano-fluid characteristics and thermal properties of Al 2 O 3 nano-particles dispersed in ethylene glycol–water mixture, International Journal of Heat and Mass Transfer 94 (2016) 262–268.

[41] W. Azmi, K. Sharma, R. Mamat, G. Najafi, M. Mohamad, The enhancement of effective thermal conductivity and effective dynamic viscosity of nanofluids–A review, Renewable and Sustainable Energy Reviews 53 (2016) 1046–1058.

[42] S. Kakaç, A. Pramuanjaroenkij, Single-phase and two-phase treatments of convective heat transfer enhancement with nanofluids–A state-of-the-art review, International Journal of Thermal Sciences 100 (2016) 75–97.

[43] G. P. Celata, F. DAnnibale, A. Mariani, L. Saraceno, R. DAmato, R. Bubbico, Heat transfer in water-based SiC and TiO_2 nanofluids, Heat Transfer Engineering 34 (13) (2013) 1060–1072.

[44] E. Chiavazzo, P. Asinari, Enhancing surface heat transfer by carbon nanofins: towards an alternative to nanofluids?, Nanoscale Research letters 6 (249).

[45] E. V. Timofeeva, W. Yu, D. M. France, D. Singh, J. L. Routbort, Nanofluids for heat transfer: an engineering approach, Nanoscale research letters 6 (1) (2011) 1–7.

[46] X.-Q. Wang, A. S. Mujumdar, A review on nanofluids-Part II: experiments and applications, Brazilian Journal of Chemical Engineering 25 (4) (2008) 631–648.

[47] S. Das, S. Choi, W. Yu, T. Pradeep, Nanofluids: Science and Technology, Wiley, 2007.

[48] P. Krajnik, F. Pusavec, A. Rashid, Nanofluids: Properties, applications and sustainability aspects in materials processing technologies, in: Advances in Sustainable Manufacturing, Springer, 107–113, 2011.

[49] L. Colla, L. Marinelli, L. Fedele, S. Bobbo, O. Manca, Characterization and Simulation of the Heat Transfer Behaviour of Water-Based ZnO Nanofluids, Journal of Nanoscience and Nanotechnology 15 (5) (2015) 3599–3609.

[50] N. Ahammed, L. G. Asirvatham, J. Titus, J. R. Bose, S. Wongwises, Measurement of thermal conductivity of graphene–water nanofluid at below and above ambient temperatures, International Communications in Heat and Mass Transfer 70 (2016) 66–74.

[51] A. Ghozatloo, A. M. Rashidi, M. Shariaty-Niasar, Effects of surface modification on the dispersion and thermal conductivity of

CNT/water nanofluids, International Communications in Heat and Mass Transfer 54 (0) (2014) 1 – 7.

[52] M. Sabiha, R. Mostafizur, R. Saidur, S. Mekhilef, Experimental investigation on thermo physical properties of single walled carbon nanotube nanofluids, International Journal of Heat and Mass Transfer 93 (2016) 862–871.

[53] C. Choi, H. Yoo, J. Oh, Preparation and heat transfer properties of nanoparticle-in-transformer oil dispersions as advanced energy-efficient coolants, Current Applied Physics 8 (6) (2008) 710–712.

[54] P. D. Shima, J. Philip, Role of Thermal Conductivity of Dispersed Nanoparticles on Heat Transfer Properties of Nanofluid, Industrial & Engineering Chemistry Research 53 (2) (2014) 980–988.

[55] W. Yu, D. M. France, J. L. Routbort, S. U. Choi, Review and comparison of nanofluid thermal conductivity and heat transfer enhancements, Heat Transfer Engineering 29 (5) (2008) 432–460.

[56] H. Akoh, Y. Tsukasaki, S. Yatsuya, A. Tasaki, Magnetic properties of ferromagnetic ultrafine particles prepared by vacuum evaporation on running oil substrate, Journal of Crystal Growth 45 (1978) 495–500.

[57] H.-t. Zhu, Y.-s. Lin, Y.-s. Yin, A novel one-step chemical method for preparation of copper nanofluids, Journal of Colloid and Interface Science 277 (1) (2004) 100–103.

[58] J. Eastman, S. Choi, S. Li, W. Yu, L. Thompson, Anomalously increased effective thermal conductivities of ethylene glycol-based

nanofluids containing copper nanoparticles, Applied Physics Letters 78 (6) (2001) 718–720.

[59] N. Nikkam, M. Saleemi, E. B. Haghighi, M. Ghanbarpour, R. Khoda-bandeh, M. Muhammed, B. Palm, M. S. Toprak, Fabrication, Characterization and Thermo-physical Property Evaluation of SiC Nanofluids for Heat Transfer Applications., Nano-Micro Letters 6 (2).

[60] N. Nikkam, M. Ghanbarpour, M. Saleemi, E. B. Haghighi, R. Khoda-bandeh, M. Muhammed, B. Palm, M. S. Toprak, Experimental investigation on thermo-physical properties of copper/diethylene glycol nanofluids fabricated via microwave-assisted route, Applied Thermal Engineering 65 (1) (2014) 158–165.

[61] Y. Zhao, J.-J. Zhu, J.-M. Hong, N. Bian, H.-Y. Chen, Microwave-Induced Polyol-Process Synthesis of Copper and Copper Oxide Nanocrystals with Controllable Morphology, European Journal of Inorganic Chemistry 2004 (20) (2004) 4072–4080.

[62] H. Bönnemann, S. Botha, B. Bladergroen, V. Linkov, Monodisperse copper-and silver-nanocolloids suitable for heat-conductive fluids, Applied organometallic chemistry 19 (6) (2005) 768–773.

[63] I. Mahbubul, R. Saidur, M. Amalina, Latest developments on the viscosity of nanofluids, International Journal of Heat and Mass Transfer 55 (4) (2012) 874 – 885.

[64] C. Granqvist, R. Buhrman, Ultrafine metal particles, Journal of Applied Physics 47 (5) (1976) 2200–2219.

[65] A. Beaber, L. Qi, J. Hafiz, P. McMurry, J. Heberlein, W. Gerberich, S. Girshick, Nanostructured SiC by chemical vapor deposition and nanoparticle impaction, Surface and Coatings Technology 202 (4) (2007) 871–875.

[66] T.-K. Hong, H.-S. Yang, C. Choi, Study of the enhanced thermal conductivity of Fe nanofluids, Journal of Applied Physics 97 (6) (2005) 064311.

[67] S. K. Das, N. Putra, W. Roetzel, Pool boiling characteristics of nano-fluids, International Journal of Heat and Mass Transfer 46 (5) (2003) 851–862.

[68] M. Chopkar, P. K. Das, I. Manna, Synthesis and characterization of nanofluid for advanced heat transfer applications, Scripta Materialia 55 (6) (2006) 549–552.

[69] B. C. Pak, Y. I. Cho, Hydrodynamic and heat transfer study of dispersed fluids with submicron metallic oxide particles, Experimental Heat Transfer: A Journal of Thermal Energy Generation, Transport, Storage, and Conversion 11 (2) (1998) 151–170.

[70] W. Yu, H. Xie, L. Chen, Y. Li, Investigation of thermal conductivity and viscosity of ethylene glycol based ZnO nanofluid, Thermochimica Acta 491 (1) (2009) 92–96.

[71] A. Abbasian Arani, J. Amani, Experimental study on the effect of TiO$_2$-Water nanofluid on heat transfer and pressure drop, Experimental Thermal and Fluid Science 42 (2012) 107–115.

[72] M. Hajipour, A. M. Dehkordi, Mixed-convection flow of Al_2O_3-H_2O nanofluid in a channel partially filled with porous metal foam: Experimental and numerical study, Experimental Thermal and Fluid Science 53 (2014) 49 – 56.

[73] L. Wang, J. Fan, Nanofluids research: key issues, Nanoscale research letters 5 (8) (2010) 1241–1252.

[74] E. Michaelides, Nanofluidics: Thermodynamic and Transport Properties, Springer, 2014.

[75] X. Li, D. Zhu, X. Wang, Evaluation on dispersion behavior of the aqueous copper nano-suspensions, Journal of colloid and interface science 310 (2) (2007) 456–463.

[76] M. P. Beck, Y. Yuan, P. Warrier, A. S. Teja, The thermal conductivity of alumina nanofluids in water, ethylene glycol, and ethylene glycol+ water mixtures, Journal of Nanoparticle research 12 (4) (2010) 1469–1477.

[77] X. Li, D. Zhu, X. Wang, N. Wang, J. Gao, H. Li, Thermal conductivity enhancement dependent pH and chemical surfactant for Cu–H_2O nanofluids, Thermochimica Acta 469 (1) (2008) 98–103.

[78] T. F. Tadros, Applied surfactants: principles and applications, John Wiley & Sons, 2006.

[79] H. Jiang, H. Li, Q. Xu, L. Shi, Effective thermal conductivity of nanofluids considering interfacial nano-shells, Materials Chemistry and Physics 148 (1) (2014) 195–200.

[80] W. Yu, S. Choi, The role of interfacial layers in the enhanced thermal conductivity of nanofluids: a renovated Maxwell model, Journal of Nanoparticle Research 5 (1-2) (2003) 167–171.

[81] W. Yu, S. Choi, The role of interfacial layers in the enhanced thermal conductivity of nanofluids: a renovated Hamilton–Crosser model, Journal of Nanoparticle Research 6 (4) (2004) 355–361.

[82] Q. Xue, W.-M. Xu, A model of thermal conductivity of nanofluids with interfacial shells, Materials Chemistry and Physics 90 (2) (2005) 298–301.

[83] L. Li, Y. Zhang, H. Ma, M. Yang, Molecular dynamics simulation of effect of liquid layering around the nanoparticle on the enhanced thermal conductivity of nanofluids, Journal of nanoparticle research 12 (3) (2010) 811–821.

[84] G. Puliti, S. Paolucci, M. Sen, Thermodynamic properties of gold–water nanolayer mixtures using molecular dynamics, Journal of Nanoparticle Research 13 (9) (2011) 4277–4293.

[85] E. Chiavazzo, M. Fasano, P. Asinari, P. Decuzzi, Scaling behaviour for the water transport in nanoconfined geometries, Nature communications 5 (4565).

[86] M. Fasano, E. Chiavazzo, P. Asinari, Water transport control in carbon nanotube arrays, Nanoscale research letters 9 (1) (2014) 1–8.

[87] M. Morciano, M. Fasano, A. Nold, C. Correia Braga, P. Yatsyshin, D. Sibley, B. Goddard, E. Chiavazzo, P. Asinari, S. Kalliadasis, Mass transfer properties of nanoconfined fluids at solid-liquid interfaces:

from atomistic simulations to continuum models, Bulletin of the American Physical Society 60 (21) (2015) 506.

[88] A. Cardellini, M. Fasano, E. Chiavazzo, P. Asinari, Mass transport phenomena at solid-liquid nanoscale interface in biomedical applications, in: VI International Conference on Computational Methods for Coupled Problems in Science and Engineering COUPLED PROBLEMS 2015, International Center for Numerical Methods in Engineering (CIMNE), 593, 2015.

[89] S. P. Jang, S. U. Choi, Role of Brownian motion in the enhanced thermal conductivity of nanofluids, Applied physics letters 84 (21) (2004) 4316–4318.

[90] J. Koo, C. Kleinstreuer, A new thermal conductivity model for nanofluids, Journal of Nanoparticle Research 6 (6) (2004) 577–588.

[91] D. H. Kumar, H. E. Patel, V. R. Kumar, T. Sundararajan, T. Pradeep, S. K. Das, Model for heat conduction in nanofluids, Physical Review Letters 93 (14) (2004) 144301.

[92] R. Prasher, P. Bhattacharya, P. E. Phelan, Thermal conductivity of nanoscale colloidal solutions (nanofluids), Physical Review Letters 94 (2) (2005) 025901.

[93] W. Evans, J. Fish, P. Keblinski, Role of Brownian motion hydrodynamics on nanofluid thermal conductivity, Applied Physics Letters 88 (9) (2006) 093116.

[94] H. E. Patel, T. Sundararajan, S. K. Das, A cell model approach for

thermal conductivity of nanofluids, Journal of Nanoparticle Research 10 (1) (2008) 87–97.

[95] R. J. Warzoha, A. S. Fleischer, Heat flow at nanoparticle interfaces, Nano Energy 6 (2014) 137–158.

[96] E. Chiavazzo, P. Asinari, Reconstruction and modeling of 3D percolation networks of carbon fillers in a polymer matrix, International Journal of Thermal Sciences 49 (2010) 2272–2281.

[97] S. A. Putnam, D. G. Cahill, B. J. Ash, L. S. Schadler, High-precision thermal conductivity measurements as a probe of polymer/nanoparticle interfaces, Journal of applied physics 94 (10) (2003) 6785–6788.

[98] R. Prasher, P. E. Phelan, P. Bhattacharya, Effect of aggregation kinetics on the thermal conductivity of nanoscale colloidal solutions (nanofluid), Nano Letters 6 (7) (2006) 1529–1534.

[99] J. Eapen, R. Rusconi, R. Piazza, S. Yip, The classical nature of thermal conduction in nanofluids, Journal of heat transfer 132 (10) (2010) 102402.

[100] C.-W. Nan, R. Birringer, D. R. Clarke, H. Gleiter, Effective thermal conductivity of particulate composites with interfacial thermal resistance, Journal of Applied Physics 81 (10) (1997) 6692–6699.

[101] R. Prasher, W. Evans, P. Meakin, J. Fish, P. Phelan, P. Keblinski, Effect of aggregation on thermal conduction in colloidal nanofluids, Applied Physics Letters 89 (14) (2006) 143119.

[102] P. Keblinski, R. Prasher, J. Eapen, Thermal conductance of nanofluids: is the controversy over?, Journal of Nanoparticle research 10 (7) (2008) 1089–1097.

[103] J. Buongiorno, D. C. Venerus, N. Prabhat, T. McKrell, J. Townsend, R. Christianson, Y. V. Tolmachev, P. Keblinski, L.-w. Hu, J. L. Alvarado, et al., A benchmark study on the thermal conductivity of nanofluids, Journal of Applied Physics 106 (9) (2009) 094312.

[104] Z. Hashin, S. Shtrikman, A variational approach to the theory of the effective magnetic permeability of multiphase materials, Journal of applied Physics 33 (10) (1962) 3125–3131.

[105] J. C. Maxwell, A treatise on electricity and magnetism, vol. 1, Clarendon press, 1873.

[106] K. D. Sattler, Handbook of Nanophysics: Nanoparticles and Quantum Dots, CRC press, 2010.

[107] B. Derjaguin, L. Landau, The theory of stability of highly charged lyophobic sols and coalescence of highly charged particles in electrolyte solutions, Acta Physicochim. URSS 14 (1941) 633–52.

[108] E. Verwey, J. T. G. Overbeek, Theory of the stability of lyophobic colloids, Journal of Colloid Science 10 (2) (1955) 224–225.

[109] R. J. Hunter, Foundations of colloid science, Oxford University Press Inc., 2001.

[110] J. N. Israelachvili, Intermolecular and surface forces: revised third edition, Academic press, 2011.

[111] G. Paul, M. Chopkar, I. Manna, P. Das, Techniques for measuring the thermal conductivity of nanofluids: a review, Renewable and Sustainable Energy Reviews 14 (7) (2010) 1913–1924.

[112] S. Lee, S.-S. Choi, S. Li, J. A. Eastman, Measuring thermal conductivity of fluids containing oxide nanoparticles, Journal of Heat Transfer 121 (2) (1999) 280–289.

[113] Y. Hwang, Y. Ahn, H. Shin, C. Lee, G. Kim, H. Park, J. Lee, Investigation on characteristics of thermal conductivity enhancement of nanofluids, Current Applied Physics 6 (6) (2006) 1068–1071.

[114] S. S. Gupta, V. M. Siva, S. Krishnan, T. Sreeprasad, P. K. Singh, T. Pradeep, S. K. Das, Thermal conductivity enhancement of nanofluids containing graphene nanosheets, Journal of Applied Physics 110 (8) (2011) 084302.

[115] C. Pang, J.-Y. Jung, J. W. Lee, Y. T. Kang, Thermal conductivity measurement of methanol-based nanofluids with Al_2O_3 and SiO_2 nanoparticles, International Journal of Heat and Mass Transfer 55 (21) (2012) 5597–5602.

[116] J. Garg, B. Poudel, M. Chiesa, J. Gordon, J. Ma, J. Wang, Z. Ren, Y. Kang, H. Ohtani, J. Nanda, et al., Enhanced thermal conductivity and viscosity of copper nanoparticles in ethylene glycol nanofluid, Journal of Applied Physics 103 (7) (2008) 074301.

[117] D. Zhu, X. Li, N. Wang, X. Wang, J. Gao, H. Li, Dispersion behavior and thermal conductivity characteristics of Al_2O_3–H_2O nanofluids, Current Applied Physics 9 (1) (2009) 131 – 139.

[118] X.-j. Wang, D.-s. Zhu, et al., Investigation of pH and SDBS on enhancement of thermal conductivity in nanofluids, Chemical Physics Letters 470 (1) (2009) 107–111.

[119] S. K. Das, N. Putra, P. Thiesen, W. Roetzel, Temperature dependence of thermal conductivity enhancement for nanofluids, Journal of Heat Transfer 125 (4) (2003) 567–574.

[120] P. Bhattacharya, S. Nara, P. Vijayan, T. Tang, W. Lai, P. Phelan, R. Prasher, D. Song, J. Wang, Characterization of the temperature oscillation technique to measure the thermal conductivity of fluids, International journal of heat and mass transfer 49 (17) (2006) 2950–2956.

[121] D.-W. Oh, A. Jain, J. K. Eaton, K. E. Goodson, J. S. Lee, Thermal conductivity measurement and sedimentation detection of aluminum oxide nanofluids by using the 3ω method, International Journal of Heat and Fluid Flow 29 (5) (2008) 1456–1461.

[122] X. Wang, X. Xu, S. U. S. Choi, Thermal conductivity of nanoparticle-fluid mixture, Journal of thermophysics and heat transfer 13 (4) (1999) 474–480.

[123] H. Kurt, M. Kayfeci, Prediction of thermal conductivity of ethylene glycol–water solutions by using artificial neural networks, Applied Energy 86 (10) (2009) 2244–2248.

[124] C. H. Li, W. Williams, J. Buongiorno, L.-W. Hu, G. Peterson, Transient and Steady-State Experimental Comparison Study of Effective

Thermal Conductivity of Al$_2$O$_3$/ Water Nanofluids, Journal of Heat Transfer 130 (4) (2008) 042407.

[125] S. W. Hong, Y.-T. Kang, C. Kleinstreuer, J. Koo, Impact analysis of natural convection on thermal conductivity measurements of nanofluids using the transient hot-wire method, International Journal of Heat and Mass Transfer 54 (15) (2011) 3448–3456.

[126] K.-C. Fang, C.-I. Weng, S.-P. Ju, An investigation into the structural features and thermal conductivity of silicon nanoparticles using molecular dynamics simulations, Nanotechnology 17 (15) (2006) 3909.

[127] M. P. Beck, Y. Yuan, P. Warrier, A. S. Teja, The effect of particle size on the thermal conductivity of alumina nanofluids, Journal of Nanoparticle Research 11 (5) (2009) 1129–1136.

[128] P. Warrier, Y. Yuan, M. P. Beck, A. S. Teja, Heat transfer in nanoparticle suspensions: modeling the thermal conductivity of nanofluids, AIChE journal 56 (12) (2010) 3243–3256.

[129] M. P. Beck, Y. Yuan, P. Warrier, A. S. Teja, The thermal conductivity of aqueous nanofluids containing ceria nanoparticles, Journal of Applied Physics 107 (6) (2010) 066101.

[130] E. V. Timofeeva, D. S. Smith, W. Yu, D. M. France, D. Singh, J. L. Routbort, Particle size and interfacial effects on thermo-physical and heat transfer characteristics of water-based α-SiC nanofluids, Nanotechnology 21 (21) (2010) 215703.

[131] M. Fasano, M. Bozorg Bigdeli, M. R. Vaziri Sereshk, E. Chiavazzo, P. Asinari, Thermal transmittance of carbon nanotube networks:

guidelines for novel thermal storage systems and polymeric material of thermal interest, Renewable and Sustainable Energy Reviews 41 (2015) 1028–1036.

[132] J. Philip, P. Shima, B. Raj, Evidence for enhanced thermal conduction through percolating structures in nanofluids, Nanotechnology 19 (30) (2008) 305706.

[133] P. Shima, J. Philip, B. Raj, Role of microconvection induced by Brownian motion of nanoparticles in the enhanced thermal conductivity of stable nanofluids, Applied Physics Letters 94 (22) (2009) 223101.

[134] T.-P. Teng, Y.-H. Hung, T.-C. Teng, H.-E. Mo, H.-G. Hsu, The effect of alumina/water nanofluid particle size on thermal conductivity, Applied Thermal Engineering 30 (1415) (2010) 2213 – 2218.

[135] M. Pastoriza-Gallego, C. Casanova, R. Páramo, B. Barbés, J. Legido, M. Piñeiro, A study on stability and thermophysical properties (density and viscosity) of Al_2O_3 in water nanofluid, Journal of Applied Physics 106 (6) (2009) 064301.

[136] C. T. Wamkam, M. K. Opoku, H. Hong, P. Smith, Effects of pH on heat transfer nanofluids containing ZrO_2 and TiO_2 nanoparticles, Journal of Applied Physics 109 (2) (2011) 024305.

[137] H. Younes, G. Christensen, X. Luan, H. Hong, P. Smith, Effects of alignment, pH, surfactant, and solvent on heat transfer nanofluids containing Fe_2O_3 and CuO nanoparticles, Journal of Applied Physics 111 (6) (2012) 064308.

[138] M. J. Ismay, E. Doroodchi, B. Moghtaderi, Effects of colloidal properties on sensible heat transfer in water-based titania nanofluids, Chemical Engineering Research and Design 91 (3) (2013) 426 – 436.

[139] D. Lee, J.-W. Kim, B. G. Kim, A new parameter to control heat transport in nanofluids: surface charge state of the particle in suspension, The Journal of Physical Chemistry B 110 (9) (2006) 4323–4328.

[140] S. W. Lee, S. D. Park, S. Kang, I. C. Bang, J. H. Kim, Investigation of viscosity and thermal conductivity of SiC nanofluids for heat transfer applications, International Journal of Heat and Mass Transfer 54 (1) (2011) 433–438.

[141] F. Cao, Y. Liu, J. Xu, Y. He, B. Hammouda, R. Qiao, B. Yang, Probing Nanoscale Thermal Transport in Surfactant Solutions, Scientific reports 5.

[142] S. Choi, Z. Zhang, W. Yu, F. Lockwood, E. Grulke, Anomalous thermal conductivity enhancement in nanotube suspensions, Applied physics letters 79 (14) (2001) 2252–2254.

[143] S. Shaikh, K. Lafdi, R. Ponnappan, Thermal conductivity improvement in carbon nanoparticle doped PAO oil: An experimental study, Journal of Applied Physics 101 (6) (2007) 064302.

[144] C. H. Li, G. Peterson, Experimental investigation of temperature and volume fraction variations on the effective thermal conductivity of nanoparticle suspensions (nanofluids), Journal of Applied Physics 99 (8) (2006) 084314.

[145] H. E. Patel, K. Anoop, T. Sundararajan, S. K. Das, A micro-convection model for thermal conductivity of nanofluids, in: International Heat Transfer Conference 13, Begel House Inc., 863–869, 2006.

[146] S. Murshed, K. Leong, C. Yang, Investigations of thermal conductivity and viscosity of nanofluids, International Journal of Thermal Sciences 47 (5) (2008) 560–568.

[147] H. A. Mintsa, G. Roy, C. T. Nguyen, D. Doucet, New temperature dependent thermal conductivity data for water-based nanofluids, International Journal of Thermal Sciences 48 (2) (2009) 363–371.

[148] R. S. Vajjha, D. K. Das, Experimental determination of thermal conductivity of three nanofluids and development of new correlations, International Journal of Heat and Mass Transfer 52 (21) (2009) 4675–4682.

[149] W. Duangthongsuk, S. Wongwises, Measurement of temperature-dependent thermal conductivity and viscosity of TiO_2–water nanofluids, Experimental Thermal and Fluid Science 33 (4) (2009) 706–714.

[150] J. Philip, P. Shima, B. Raj, Nanofluid with tunable thermal properties, Applied Physics Letters 92 (4) (2008) 043108–043108.

[151] P. Shima, J. Philip, B. Raj, Magnetically controllable nanofluid with tunable thermal conductivity and viscosity, Applied physics letters 95 (13) (2009) 133112–133112.

[152] J. A. Eastman, S. Phillpot, S. Choi, P. Keblinski, Thermal transport in nanofluids 1, Annu. Rev. Mater. Res. 34 (2004) 219–246.

[153] H. E. Patel, T. Sundararajan, S. K. Das, An experimental investigation into the thermal conductivity enhancement in oxide and metallic nanofluids, Journal of Nanoparticle Research 12 (3) (2010) 1015–1031.

[154] A. Ijam, R. Saidur, Nanofluid as a coolant for electronic devices (cooling of electronic devices), Applied Thermal Engineering 32 (2012) 76–82.

[155] M. Liu, M. C. Lin, C. Wang, Enhancements of thermal conductivities with Cu, CuO, and carbon nanotube nanofluids and application of MWNT/water nanofluid on a water chiller system, Nanoscale research letters 6 (1) (2011) 1–13.

[156] Y. Hwang, H. Park, J. Lee, W. Jung, Thermal conductivity and lubrication characteristics of nanofluids, Current Applied Physics 6 (2006) e67–e71.

[157] N. Nikkam, E. B. Haghighi, M. Saleemi, M. Behi, R. Khodabandeh, M. Muhammed, B. Palm, M. S. Toprak, Experimental study on preparation and base liquid effect on thermo-physical and heat transport characteristics of α-SiC nanofluids, International Communications in Heat and Mass Transfer 55 (2014) 38–44.

[158] E. V. Timofeeva, A. N. Gavrilov, J. M. McCloskey, Y. V. Tolmachev, S. Sprunt, L. M. Lopatina, J. V. Selinger, Thermal conductivity and particle agglomeration in alumina nanofluids: experiment and theory, Physical Review E 76 (6) (2007) 061203.

[159] R. G. Jackson, M. Kahani, N. Karwa, A. Wu, R. Lamb, R. Taylor, G. Rosengarten, Effect of surface wettability on carbon nanotube

water-based nanofluid droplet impingement heat transfer, in: Journal of Physics: Conference Series, vol. 525, IOP Publishing, 012024, 2014.

[160] S. Harish, K. Ishikawa, E. Einarsson, S. Aikawa, T. Inoue, P. Zhao, M. Watanabe, S. Chiashi, J. Shiomi, S. Maruyama, Temperature Dependent Thermal Conductivity Increase of Aqueous Nanofluid with Single Walled Carbon Nanotube Inclusion, Materials Express 2 (3) (2012) 213–223.

[161] M. Corcione, Empirical correlating equations for predicting the effective thermal conductivity and dynamic viscosity of nanofluids, Energy Conversion and Management 52 (1) (2011) 789–793.

[162] C. H. Chon, K. D. Kihm, S. P. Lee, S. U. Choi, Empirical correlation finding the role of temperature and particle size for nanofluid (Al_2O_3) thermal conductivity enhancement, Applied Physics Letters 87 (15) (2005) 153107–153107.

[163] E. V. Timofeeva, J. L. Routbort, D. Singh, Particle shape effects on thermophysical properties of alumina nanofluids, Journal of Applied Physics 106 (1) (2009) 014304.

[164] C. Pang, J. W. Lee, H. Hong, Y. T. Kang, Heat conduction mechanism in nanofluids, Journal of Mechanical Science and Technology 28 (7) (2014) 2925–2936.

[165] K. Khanafer, K. Vafai, A critical synthesis of thermophysical characteristics of nanofluids, International Journal of Heat and Mass Transfer 54 (19-20) (2011) 4410–4428.

[166] R. Hamilton, O. Crosser, Thermal conductivity of heterogeneous two-component systems, Industrial & Engineering chemistry fundamentals 1 (3) (1962) 187–191.

[167] D. J. Jeffrey, Conduction through a random suspension of spheres, Proceedings of the Royal Society of London. A. Mathematical and Physical Sciences 335 (1602) (1973) 355–367.

[168] R. Vajjha, D. Das, P. Namburu, Numerical study of fluid dynamic and heat transfer performance of Al_2O_3 and CuO nanofluids in the flat tubes of a radiator, International Journal of Heat and Fluid Flow 31 (4) (2010) 613–621.

[169] M. Corcione, Rayleigh-Bnard convection heat transfer in nanoparticle suspensions, International Journal of Heat and Fluid Flow 32 (1) (2011) 65 – 77.

[170] A. Ghadimi, R. Saidur, H. Metselaar, A review of nanofluid stability properties and characterization in stationary conditions, International Journal of Heat and Mass Transfer 54 (1718) (2011) 4051 – 4068.

[171] A. Rajabpour, F. Y. Akizi, M. M. Heyhat, K. Gordiz, Molecular dynamics simulation of the specific heat capacity of water-Cu nanofluids, International Nano Letters 3 (1) (2013) 58.

[172] Y. Yang, Z. G. Zhang, E. A. Grulke, W. B. Anderson, G. Wu, Heat transfer properties of nanoparticle-in-fluid dispersions (nanofluids) in laminar flow, International Journal of Heat and Mass Transfer 48 (6) (2005) 1107 – 1116.

[173] S.-Q. Zhou, R. Ni, Measurement of the specific heat capacity of water-based Al_2O_3 nanofluid, Applied Physics Letters 92 (9) (2008) 093123–093123.

[174] M. Pantzali, A. Kanaris, K. Antoniadis, A. Mouza, S. Paras, Effect of nanofluids on the performance of a miniature plate heat exchanger with modulated surface, International Journal of Heat and Fluid Flow 30 (4) (2009) 691–699.

[175] A. K. Starace, J. C. Gomez, J. Wang, S. Pradhan, G. C. Glatzmaier, Nanofluid heat capacities, Journal of Applied Physics 110 (12) (2011) 124323.

[176] V. Kumaresan, R. Velraj, Experimental investigation of the thermo-physical properties of water–ethylene glycol mixture based CNT nanofluids, Thermochimica Acta 545 (2012) 180–186.

[177] M. Saeedinia, M. Akhavan-Behabadi, P. Razi, Thermal and rheological characteristics of CuO–Base oil nanofluid flow inside a circular tube, International Communications in Heat and Mass Transfer 39 (1) (2012) 152–159.

[178] M. Elias, I. Mahbubul, R. Saidur, M. Sohel, I. Shahrul, S. Khaleduzzaman, S. Sadeghipour, Experimental investigation on the thermo-physical properties of Al_2O_3 nanoparticles suspended in car radiator coolant, International Communications in Heat and Mass Transfer 54 (2014) 48–53.

[179] R. S. Vajjha, D. K. Das, Specific heat measurement of three nanofluids

77

and development of new correlations, Journal of heat transfer 131 (7) (2009) 071601.

[180] S. S. Murshed, Simultaneous measurement of thermal conductivity, thermal diffusivity, and specific heat of nanofluids, Heat Transfer Engineering 33 (8) (2012) 722–731.

[181] D. P. Kulkarni, R. S. Vajjha, D. K. Das, D. Oliva, Application of aluminum oxide nanofluids in diesel electric generator as jacket water coolant, Applied Thermal Engineering 28 (14) (2008) 1774–1781.

[182] M. Fakoor Pakdaman, M. Akhavan-Behabadi, P. Razi, An experimental investigation on thermo-physical properties and overall performance of MWCNT/heat transfer oil nanofluid flow inside vertical helically coiled tubes, Experimental Thermal and Fluid Science 40 (2012) 103–111.

[183] S. D. Pandey, V. Nema, Experimental analysis of heat transfer and friction factor of nanofluid as a coolant in a corrugated plate heat exchanger, Experimental Thermal and Fluid Science 38 (2012) 248–256.

[184] E. D. Robertis, E. Cosme, R. Neves, A. Kuznetsov, A. Campos, S. Landi, C. Achete, Application of the modulated temperature differential scanning calorimetry technique for the determination of the specific heat of copper nanofluids, Applied Thermal Engineering 41 (0) (2012) 10 – 17, 13th Brazilian Congress of Thermal Sciences and Engineering.

[185] B.-X. Wang, L.-P. Zhou, X.-F. Peng, Surface and size effects on the

specific heat capacity of nanoparticles, International journal of thermophysics 27 (1) (2006) 139–151.

[186] Q. He, S. Wang, M. Tong, Y. Liu, Experimental study on thermophysical properties of nanofluids as phase-change material (PCM) in low temperature cool storage, Energy Conversion and Management 64 (2012) 199–205.

[187] I. Shahrul, I. Mahbubul, S. Khaleduzzaman, R. Saidur, M. Sabri, A comparative review on the specific heat of nanofluids for energy perspective, Renewable and Sustainable Energy Reviews 38 (2014) 88–98.

[188] A. Amrollahi, A. Hamidi, A. Rashidi, The effects of temperature, volume fraction and vibration time on the thermo-physical properties of a carbon nanotube suspension (carbon nanofluid), Nanotechnology 19 (31) (2008) 315701.

[189] Y. Xuan, W. Roetzel, Conceptions for heat transfer correlation of nanofluids, International Journal of Heat and Mass Transfer 43 (19) (2000) 3701–3707.

[190] H. O'Hanley, J. Buongiorno, T. McKrell, L.-w. Hu, Measurement and model validation of nanofluid specific heat capacity with differential scanning calorimetry, Advances in Mechanical Engineering 2012.

[191] S. S. Murshed, Determination of effective specific heat of nanofluids, Journal of Experimental Nanoscience 6 (5) (2011) 539–546.

[192] T.-P. Teng, Y.-H. Hung, Estimation and experimental study of the density and specific heat for alumina nanofluid, Journal of Experimental Nanoscience 9 (7) (2012) 707–718.

[193] C.-J. Ho, M. Chen, Z. Li, Numerical simulation of natural convection of nanofluid in a square enclosure: effects due to uncertainties of viscosity and thermal conductivity, International Journal of Heat and Mass Transfer 51 (17) (2008) 4506–4516.

[194] K. Khanafer, K. Vafai, M. Lightstone, Buoyancy-driven heat transfer enhancement in a two-dimensional enclosure utilizing nanofluids, International Journal of Heat and Mass Transfer 46 (19) (2003) 3639–3653.

[195] C. Ho, W. Liu, Y. Chang, C. Lin, Natural convection heat transfer of alumina-water nanofluid in vertical square enclosures: an experimental study, International Journal of Thermal Sciences 49 (8) (2010) 1345–1353.

[196] M. Chandrasekar, S. Suresh, A. Chandra Bose, Experimental investigations and theoretical determination of thermal conductivity and viscosity of Al_2O_3/water nanofluid, Experimental Thermal and Fluid Science 34 (2) (2010) 210–216.

[197] W. Xian-Ju, L. Xin-Fang, Influence of pH on Nanofluids' Viscosity and Thermal Conductivity, Chinese Physics Letters 26 (5) (2009) 056601.

[198] C. Nguyen, F. Desgranges, G. Roy, N. Galanis, T. Mar, S. Boucher, H. Angue Mintsa, Temperature and particle-size dependent viscosity data for water-based nanofluids - Hysteresis phenomenon, International Journal of Heat and Fluid Flow 28 (6) (2007) 1492–1506.

[199] Y. J. Kang, S. Yang, Integrated microfluidic viscometer equipped with

fluid temperature controller for measurement of viscosity in complex fluids, Microfluidics and nanofluidics 14 (3-4) (2013) 657–668.

[200] A. Einstein, Eine neue bestimmung der moleküldimensionen, Annalen der Physik 324 (2) (1906) 289–306.

[201] I. M. Krieger, T. J. Dougherty, A mechanism for non-Newtonian flow in suspensions of rigid spheres, Transactions of the Society of Rheology 3 (1) (1959) 137–152.

[202] V. Egan, P. Walsh, E. Walsh, On viscosity measurements of nanofluids in micro and mini tube flow, Journal of Physics D: Applied Physics 42 (16) (2009) 165502.

[203] S. P. Jang, J.-H. Lee, K. S. Hwang, S. U. Choi, Particle concentration and tube size dependence of viscosities of Al_2O_3–water nanofluids flowing through micro-and minitubes, Applied Physics Letters 91 (24) (2007) 243112–243112.

[204] F. Ayela, J. Chevalier, Comment on Particle concentration and tube size dependence of viscosities of Al_2O_3–water nanofluids flowing through micro-and minitubes[Appl. Phys. Lett. 91, 243112 (2007)], Applied Physics Letters 94 (6) (2009) 066101–066101.

[205] D. R. Heine, M. K. Petersen, G. S. Grest, Effect of particle shape and charge on bulk rheology of nanoparticle suspensions, The Journal of Chemical Physics 132 (18) (2010) 184509.

[206] I. Santamara-Holek, C. I. Mendoza, The rheology of concentrated suspensions of arbitrarily-shaped particles, Journal of Colloid and Interface Science 346 (1) (2010) 118 – 126.

[207] Y. Rao, Nanofluids: Stability, phase diagram, rheology and applications, Particuology 8 (6) (2010) 549 – 555.

[208] R. Prasher, D. Song, J. Wang, P. Phelan, Measurements of nanofluid viscosity and its implications for thermal applications, Applied Physics Letters 89 (13) (2006) 133108.

[209] J. B. Mena, A. A. Ubices de Moraes, Y. R. Benito, G. Ribatski, J. A. R. Parise, Extrapolation of Al_2O_3–water nanofluid viscosity for temperatures and volume concentrations beyond the range of validity of existing correlations, Applied Thermal Engineering 51 (1) (2013) 1092–1097.

[210] W. Yu, H. Xie, Y. Li, L. Chen, Experimental investigation on thermal conductivity and viscosity of aluminum nitride nanofluid, Particuology 9 (2) (2011) 187 – 191.

[211] S. Kim, C. Kim, W.-H. Lee, S.-R. Park, Rheological properties of alumina nanofluids and their implication to the heat transfer enhancement mechanism, Journal of Applied Physics 110 (3) (2011) 034316.

[212] T. X. Phuoc, M. Massoudi, R.-H. Chen, Viscosity and thermal conductivity of nanofluids containing multi-walled carbon nanotubes stabilized by chitosan, International Journal of Thermal Sciences 50 (1) (2011) 12–18.

[213] Z. Mingzheng, X. Guodong, L. Jian, C. Lei, Z. Lijun, Analysis of factors influencing thermal conductivity and viscosity in different kinds of surfactant solutions, Experimental Thermal and Fluid Science 36 (0) (2012) 22 – 29.

[214] E. V. Timofeeva, M. R. Moravek, D. Singh, Improving the heat transfer efficiency of synthetic oil with silica nanoparticles, Journal of colloid and interface science 364 (1) (2011) 71–79.

[215] P. Kamranfar, M. Jamialahmadi, Effect of surfactant micelle shape transition on the microemulsion viscosity and its application in enhanced oil recovery processes, Journal of Molecular Liquids .

[216] C. Nguyen, F. Desgranges, N. Galanis, G. Roy, T. Maré, S. Boucher, H. Angue Mintsa, Viscosity data for Al_2O_3–water nanofluid–hysteresis: is heat transfer enhancement using nanofluids reliable?, International Journal of Thermal Sciences 47 (2) (2008) 103–111.

[217] W.-Q. Lu, Q.-M. Fan, Study for the particle's scale effect on some thermophysical properties of nanofluids by a simplified molecular dynamics method, Engineering Analysis with Boundary Elements 32 (4) (2008) 282–289.

[218] M. Pastoriza-Gallego, C. Casanova, J. Legido, M. Pieiro, CuO in water nanofluid: Influence of particle size and polydispersity on volumetric behaviour and viscosity, Fluid Phase Equilibria 300 (12) (2011) 188 – 196.

[219] V. Y. Rudyak, S. Krasnolutskii, Dependence of the viscosity of nanofluids on nanoparticle size and material, Physics Letters A 378 (26) (2014) 1845–1849.

[220] Y. He, Y. Jin, H. Chen, Y. Ding, D. Cang, H. Lu, Heat transfer and flow behaviour of aqueous suspensions of TiO_2 nanoparticles (nanoflu-

ids) flowing upward through a vertical pipe, International Journal of Heat and Mass Transfer 50 (11-12) (2007) 2272–2281.

[221] B. C. Sahoo, R. S. Vajjha, R. Ganguli, G. A. Chukwu, D. K. Das, Determination of rheological behavior of aluminum oxide nanofluid and development of new viscosity correlations, Petroleum Science and Technology 27 (15) (2009) 1757–1770.

[222] L. Godson, B. Raja, D. M. Lal, S. Wongwises, Experimental investigation on the thermal conductivity and viscosity of silver-deionized water nanofluid, Experimental Heat Transfer 23 (4) (2010) 317–332.

[223] M. Hemmat Esfe, S. Saedodin, An experimental investigation and new correlation of viscosity of ZnO–EG nanofluid at various temperatures and different solid volume fractions, Experimental Thermal and Fluid Science 55 (2014) 1–5.

[224] M. Ghanbarpour, E. Bitaraf Haghigi, R. Khodabandeh, Thermal properties and rheological behavior of water based Al_2O_3 nanofluid as a heat transfer fluid, Experimental Thermal and Fluid Science 53 (2014) 227–235.

[225] M. K. Meybodi, A. Daryasafar, M. M. Koochi, J. Moghadasi, R. B. Meybodi, A. K. Ghahfarokhi, A novel correlation approach for viscosity prediction of water based nanofluids of Al2O3, TiO2, SiO2 and CuO, Journal of the Taiwan Institute of Chemical Engineers 58 (2016) 19–27.

[226] W. J. Tseng, K.-C. Lin, Rheology and colloidal structure of aqueous

TiO$_2$ nanoparticle suspensions, Materials Science and Engineering: A 355 (12) (2003) 186 – 192.

[227] P. Namburu, D. Kulkarni, A. Dandekar, D. Das, Experimental investigation of viscosity and specific heat of silicon dioxide nanofluids, Micro & Nano Letters, IET 2 (3) (2007) 67–71.

[228] D. P. Kulkarni, D. K. Das, R. S. Vajjha, Application of nanofluids in heating buildings and reducing pollution, Applied Energy 86 (12) (2009) 2566 – 2573.

[229] P. K. Namburu, D. P. Kulkarni, D. Misra, D. K. Das, Viscosity of copper oxide nanoparticles dispersed in ethylene glycol and water mixture, Experimental Thermal and Fluid Science 32 (2) (2007) 397–402.

[230] N. Putra, W. Roetzel, S. K. Das, Natural convection of nano-fluids, Heat and Mass Transfer 39 (8-9) (2003) 775–784.

[231] K. Anoop, S. Kabelac, T. Sundararajan, S. K. Das, Rheological and flow characteristics of nanofluids: Influence of electroviscous effects and particle agglomeration, Journal of applied physics 106 (3) (2009) 034909.

[232] G. Batchelor, The effect of Brownian motion on the bulk stress in a suspension of spherical particles, Journal of Fluid Mechanics 83 (01) (1977) 97–117.

[233] H. C. Brinkman, The Viscosity of Concentrated Suspensions and Solutions, The Journal of Chemical Physics 20 (4) (1952) 571–571.

[234] T. S. Lundgren, Slow flow through stationary random beds and suspensions of spheres, Journal of Fluid Mechanics 51 (02) (1972) 273–299.

[235] N. Frankel, A. Acrivos, On the viscosity of a concentrated suspension of solid spheres, Chemical Engineering Science 22 (6) (1967) 847–853.

[236] H. Chen, Y. Ding, Y. He, C. Tan, Rheological behaviour of ethylene glycol based titania nanofluids, Chemical Physics Letters 444 (4-6) (2007) 333–337, cited By (since 1996)105.

[237] T. Kitano, T. Kataoka, T. Shirota, An empirical equation of the relative viscosity of polymer melts filled with various inorganic fillers, Rheologica Acta 20 (2) (1981) 207–209.

[238] A. L. Graham, On the viscosity of suspensions of solid spheres, Applied Scientific Research 37 (3-4) (1981) 275–286.

[239] N. Masoumi, N. Sohrabi, A. Behzadmehr, A new model for calculating the effective viscosity of nanofluids, Journal of Physics D: Applied Physics 42 (5) (2009) 055501.

[240] G. A. Longo, C. Zilio, E. Ceseracciu, M. Reggiani, Application of artificial neural network (ANN) for the prediction of thermal conductivity of oxide–water nanofluids, Nano Energy 1 (2) (2012) 290–296.

[241] R. Vajjha, D. Das, B. Mahagaonkar, Density measurement of different nanofluids and their comparison with theory, Petroleum Science and Technology 27 (6) (2009) 612–624.

[242] A. A. Servati V, K. Javaherdeh, H. R. Ashorynejad, Magnetic field effects on force convection flow of a nanofluid in a channel partially

filled with porous media using Lattice Boltzmann Method, Advanced Powder Technology 25 (2) (2014) 666–675.

[243] F. P. Incropera, Liquid cooling of electronic devices by single-phase convection, vol. 3, Wiley-Interscience, 1999.

[244] A. ASHRAE, Handbook of fundamentals, American Society of Heating Refrigerating and Air Conditioning Engineers, Atlanta, GA .

[245] F. McQuiston, J. Parker, J. Spitler, Heating, Ventilating, and Air Conditioning: Analysis and Design, John Wiley & Sons, 2005.

[246] V. Bianco, S. Nardini, O. Manca, Enhancement of heat transfer and entropy generation analysis of nanofluids turbulent convection flow in square section tubes, Nanoscale research letters 6 (1) (2011) 1–12.

[247] Y. Li, J. Fernández-Seara, K. Du, Á. Á. Pardiñas, L. L. Latas, W. Jiang, Experimental investigation on heat transfer and pressure drop of ZnO/ethylene glycol-water nanofluids in transition flow, Applied Thermal Engineering 93 (2016) 537–548.

[248] P. Razi, M. Akhavan-Behabadi, M. Saeedinia, Pressure drop and thermal characteristics of CuO–base oil nanofluid laminar flow in flattened tubes under constant heat flux, International Communications in Heat and Mass Transfer 38 (7) (2011) 964 – 971.

[249] A. Bejan, Heat transfer, 1993, John Wiely & Sons Inc .

[250] V. Gnielinski, New equations for heat and mass-transfer in turbulent pipe and channel flow, International Chemical Engineering 16 (2) (1976) 359–368.

[251] R. S. Vajjha, D. K. Das, D. P. Kulkarni, Development of new correlations for convective heat transfer and friction factor in turbulent regime for nanofluids, International Journal of Heat and Mass Transfer 53 (21) (2010) 4607–4618.

[252] S. Ferrouillat, A. Bontemps, O. Poncelet, O. Soriano, J.-A. Gruss, Influence of nanoparticle shape factor on convective heat transfer and energetic performance of water-based SiO_2 and ZnO nanofluids, Applied Thermal Engineering 51 (1) (2013) 839–851.

[253] M. Bai, Z. Xu, J. Lv, Application of Nanofluids in Engine Cooling System, Tech. Rep., SAE Technical Paper, 2008.

[254] S. Peyghambarzadeh, S. Hashemabadi, S. Hoseini, M. Seifi Jamnani, Experimental study of heat transfer enhancement using water/ethylene glycol based nanofluids as a new coolant for car radiators, International Communications in Heat and Mass Transfer 38 (9) (2011) 1283–1290.

[255] G. Huminic, A. Huminic, Numerical analysis of laminar flow heat transfer of nanofluids in a flattened tube, International Communications in Heat and Mass Transfer 44 (0) (2013) 52 – 57.

[256] A. M. Hussein, R. Bakar, K. Kadirgama, K. Sharma, Experimental measurement of nanofluids thermal properties, Diamond 380 (237) (2013) 390.

[257] W. Ailor, Engine Coolant Testing: State of the Art, ASTM STP 705, American Society for Testing and Materials, 1980.

[258] A. Ghadimi, I. H. Metselaar, The influence of surfactant and ultrasonic processing on improvement of stability, thermal conductivity and viscosity of titania nanofluid, Experimental Thermal and Fluid Science 51 (2013) 1–9.